Lipids Maintain Genomic Stability and Developmental Potency of Murine Pluripotent Stem Cells

Liangwen Zhong[1], Miriam Gordillo[2,7], Xingyi Wang[4,7], Yiren Qin[1,7], Yuanyuan Huang[1], Alexey Soshnev[3], Ritu Kumar[6], Gouri Nanjangud[5], Daylon James[1], C. David Allis[3], Todd Evans[2,*], Bryce Carey[3,*], Duancheng Wen[1,*]

[1]Ronald O. Perelman and Claudia Cohen Center for Reproductive Medicine, Weill Cornell Medicine, New York, NY 10065, USA

[2]Department of Surgery, Weill Cornell Medical College, 1300 York Avenue, New York, NY 10065, USA

[3]Laboratory of Chromatin Biology & Epigenetics, The Rockefeller University, New York, NY 10065, USA

[4]Cold Spring Harbor Laboratory, Cold Spring Harbor, NY 11724, USA.

[5]Molecular Cytogenetics Core. Memorial Sloan Kettering Cancer Center, New York, New York 10065, USA

[6]Gladstone Institutes, 1650 Owens St, San Francisco, CA 94158, USA

[7]These authors contributed equally

*Correspondence should be addressed to:

Duancheng Wen, Ph.D., Email: duw2001@med.cornell.edu;

Bryce Carey, Ph.D., Email: bwcarey@gmail.com

Todd Evans, Ph.D., Email: tre2003@med.cornell.edu

ABSTRACT: Lipids play vital roles in cellular homeostasis and regulate pluripotency of human stem cells. However, the impact of lipids on murine pluripotent stem cells is unclear. While Mek1/2 and Gsk3β inhibition ("2i") supports the maintenance of murine embryonic stem cells (ESCs) in a homogenous naïve state, prolonged culture in 2i results in aneuploidy and DNA hypomethylation that impairs developmental potential. Additionally, 2i fails to support derivation and culture of fully potent female ESCs. Here we find that mouse ESCs cultured in 2i/LIF supplemented with lipid-rich albumin (AlbuMAX) undergo pluripotency transition yet maintain genomic stability and full potency over long-term culture. Mechanistically, lipids in AlbuMAX impact intracellular metabolism including nucleotide biosynthesis, lipid biogenesis, and TCA cycle intermediates, with enhanced expression of ZCAN4 and DNMT3s that prevent telomere shortening and DNA hypomethylation. In concert with 2i, lipids induce a formative-like pluripotent state through direct stimulation of Mek-mediated Erk2 phosphorylation, which also alleviates X chromosome loss in female ESCs. Importantly, both male and female "all-ESC" mice can be generated from *de novo* derived ESCs using AlbuMAX-based media. Our findings underscore the importance of lipids to pluripotency and link nutrient cues to genome integrity in early development.

Key words: Mouse pluripotent stem cells, Lipids, Pluripotency transition, Genomic stability, Developmental potency, Naïve pluripotency, Formative-like pluripotency, Nucleotide pool depletion, Telomere shortening, Erk1/2 signaling, 2i medium, X chromosome loss, Female all-ESC mice

42 **INTRODUCTION**

43 Lipids play vital roles in the maintenance of cellular homeostasis by serving as an
44 energy source through mitochondrial fatty acid oxidation, enhancing intracellular signal
45 transduction, and providing macromolecules for membrane biosynthesis during growth
46 and proliferation [1]. Lipids also affect stem cell pluripotency as demonstrated in recent
47 reports that lipid supplementation in E8 medium induces differentiation of intermediate
48 human ESCs into a primed stage [2, 3] and regulate human ESCs self-renewal [4].
49 However, the role of lipids on murine pluripotent stem cells is still poorly understood.

50 Pluripotency is the ability of a single cell to generate all cell lineages of an adult
51 animal. Pluripotent murine ESCs were initially derived in media supplemented with fetal
52 bovine serum (FBS) on feeder layers of mouse embryonic fibroblasts [5, 6]. Yet
53 undefined serum components results in heterogeneous cultures and gradual loss of
54 pluripotency [7]. The breakthrough discovery that inhibition of Mek1/2 and Gsk3β (2i)
55 maintains murine ESCs in a more homogenous state of naive pluripotency [8], enabled
56 stabilization and expansion of ground state ESCs *in vitro.* Recently, pluripotency has
57 been described as a developmental continuum including three distinct phases: naïve,
58 formative, and primed states, which correlate with murine embryonic stem cells
59 (mESCs), formative pluripotent stem cells (fPSCs), and epiblast stem cells (EpiSCs),
60 respectively [7-14]. Murine ESCs derived from the inner cell mass of E3.5-E4.5
61 blastocysts have unlimited self-renewal and differentiation capacity [5, 6, 8], as
62 evidenced by their ability to generate all-ESC mice in tetraploid complementation
63 assays [15-18]. Murine EpiSCs derived from post implantation epiblasts (E5.5–E8.25)

are lineage primed for differentiation; their developmental potential is limited as they are unable to colonize blastocyst embryos [13, 14, 19, 20]. The recently proposed fPSCs are derived from E5.5-E6.5 embryos and are thought to possess unrestricted developmental potential. However, this has not been formally demonstrated, as the cells cannot be transitioned to a naïve state and they are less efficient compared to naïve cells for chimera contribution [9, 21, 22]. In these reports the fPSCs were derived by manipulating Activin A and Wnt signaling pathways, which may have different response thresholds for different PSC lines.

Defined serum-free 2i/LIF medium, which has been widely used in stem cell research, enables derivation of ESC lines from non-permissive strains that cannot be generated using serum-containing media [23-27]. Recently, however, two groups reported that prolonged culture of murine ESCs in 2i/LIF medium results in aneuploidy, loss of DNA methylation, and impaired developmental potential; moreover, the 2i/LIF system does not support the derivation of fully potent female ESCs [28, 29], suggesting a new approach is needed for deriving and maintaining stable ESCs of both sexes with full developmental potential.

Here, we provide definitive evidence that lipid supplementation (AlbuMAX, AX) maintains genomic stability and developmental potency over long term culture, and drives pluripotency transition through activated Erk signaling, which also supports female ESC X chromosome stability. Importantly, AX-induced formative-like ESCs are reversible by manipulating Fgf/Erk signaling, and AX-based medium is beneficial for both male and female ESC derivation, for culture and maintenance of full developmental potency in outbred or inbred strains.

87 **RESULTS**

88 **AX improves developmental potential of murine ESCs**

89 Murine naïve stem cells are maintained in a serum-free medium supplemented with
90 GSK3β and Mek inhibitors (PD184352 and CHIR99021, 2i) and leukemia inhibitory
91 factor (LIF) [8] (hereafter 2iL for the 2i/LIF medium or 2i-ESCs for the ESCs cultured in
92 2i/LIF medium). To test how lipids can influence pluripotent stem cells in serum-free
93 media conditions, a chromatographically purified lipid-rich bovine serum albumin,
94 AlbuMAX (A or AX), was added to 2iL culture medium (hereafter 2iLA for 2i/LIF+
95 AlbuMAX medium or AX-ESCs for ESCs cultured in 2iLA medium) (**Fig. 1a**). Male ESCs
96 cultured in 2iLA medium maintained bright but flatter/larger colonies for over 15
97 passages, whereas the colonies in 2iL medium without AX acquired a flat and dark
98 appearance (**Fig. 1b and Extended data Fig. 1a**). ESCs cultured in 2iLA proliferated
99 more rapidly than in 2iL with doubling time at early passages (p3-p5) of 6.7h compared
100 to 10.2h, respectively (**Extended data Fig. 1a**). Over continued passaging, the
101 proliferation of AX-ESCs gradually slowed with doubling time increasing to 8.1h at
102 passage 15 and reaching to 10.7h at passage 20 (**Extended data Fig. 1a**).

103 After injection into blastocyst embryos, AX-ESCs gave rise to post-natal chimeras
104 with germline transmission (**Extended data Fig. 1b).** To test for full developmental
105 potency, AX-ESCs were assayed for the ability to generate all-ESC mice by tetraploid
106 complementation. Both 2i-ESCs and AX-ESCs could generate all-ESC mice at high
107 efficiency in early passages (p1–5) (**Fig.1c**). Consistent with previous studies [28, 29],
108 prolonged culture of ESCs in 2iL demonstrated loss of developmental potential by 15
109 passages. Intriguingly, ESCs cultured in 2iLA medium retained the potential to generate

110 all-ESC mice for over 20 passages (**Fig. 1c and Extended data Fig. 1c, 1d**). We
111 frequently obtained as many as seven full-term live pups from a single surrogate mother
112 (**Fig. 1c and Extended data Fig.1c),** efficiency similar to early passage 2i-ESCs.
113 Although the potential for AX-ESCs to generate all-ESC mice decreased over time, it
114 extended to passage 43 after 3 months of culture **(Fig. 1c and Extended data Fig. 1e)**.

115 **AX promotes karyotypic stability in ESC cultures**

116 Because aneuploidy is the leading genetic cause of early pregnancy loss [30], we
117 speculated that improved developmental potential of AX-ESCs may be due to improved
118 genomic stability. We analyzed the karyotypes of ESCs cultured in 2iL and 2iLA media.
119 Over 85% of ESCs cultured in either 2iL or 2iLA showed normal karyotype (40, XY) at
120 passage 3 (P3), but by passage 15-25, nearly 95% of the cells maintained in 2iL
121 exhibited aneuploidy (**Fig. 1d**), with trisomy 8 prevailing among aneuploid cells
122 (**Extended data Fig. 2a-c**). By passage 43 nearly 100% of cells displayed aneuploidy,
123 with a high prevalence of chromosome loss (**Fig. 1d-e, Extended data Fig. 2d-e**).
124 Many of these ESCs had reduced chromosome content that approached haploid
125 karyotype (**Fig. 1e and Extended data Fig. 2d-2e**). Remarkably, ESCs cultured in 2iLA
126 medium had significantly higher number of cells exhibiting a normal karyotype, with over
127 68.3%, 50%, and 16.7% at passages 15, 25, and 43, respectively (**Fig. 1d**) indicating
128 increased genome stability in cells grown in 2iLA. In addition, unlike 2i-ESCs, AX-ESCs
129 maintained a near diploid karyotype (**Extended data Fig. 2d-2e)**. Female ESCs tend to
130 quickly loss one of their two X chromosomes in 2iL medium [28, 29], so a dual reporter
131 female ESC line ($X^{GFP}X^{Tomato}$, $X^{G}X^{T}$) [28] was employed to measure X chromosome loss
132 by flow cytometry. Consistent with increased genomic instability, approximately 40% of

133 cells at passage 10, and over 90% at passage 15, lost one X chromosome in ESCs
134 cultured in 2iL medium (**Fig. 1f**). Notably, ESCs in 2iLA medium maintained two X
135 chromosomes in over 95% of the cells with very little fluctuation from passage 3 to
136 passage 15 (**Fig. 1f**). Karyotyping of the X^GX^T ESCs at P15 confirmed the physical loss
137 of X chromosome in 2i-ESCs and thus excluded the possibility of X chromosome
138 inactivation in 2iL medium (**Fig. 1g**). Together, these data suggest that AX can
139 efficiently prevent X chromosome loss in female ESCs and promotes karyotypic stability
140 in ESC cultures.

141 **AX prevents nucleotide pool depletion and telomere shortening in 2iL medium**

142 The reduced chromosome content of cultured 2i-ESCs (**Fig. 1e and Extended data**
143 **Fig. 2d-2e**), indicates a possible deficiency in DNA replication and repair, which could
144 be caused by imbalanced endogenous nucleotide pools [31-33]. We performed liquid
145 chromatography-mass spectrometry (LC-MS) comparing ESCs cultured in 2iL or 2iLA
146 conditions. Steady-state endogenous nucleotide pools are severely depleted in 2i-ESCs
147 compared to AX-ESCs (**Fig. 1h**). Most of the nucleotides including thymidine, 2'-
148 deoxyguanosine, 2'-deoxyinosine, and the precursor aspartate, are dramatically
149 reduced in 2i-ESCs. Speculating that nucleotide biosynthesis pathways are impacted in
150 2iL medium, resulting in depletion of endogenous nucleotide pools, we analyzed the
151 expression of Prps2, an ATP-dependent enzyme in the syntheses
152 of purines and pyrimidines from ribose 5-phosphate [34, 35]. Real-time quantitative RT-
153 PCR (qPCR) and western blotting analyses showed that Prps2 is expressed at
154 significantly lower levels in 2i-ESCs compared to AX-ESCs (**Fig. 1i**), supporting the

155 hypothesis that nucleotide biosynthesis is attenuated in 2iL medium and maintained by
156 AX supplementation.

157 Decreasing dNTP (nucleotide) levels can lead to telomere shortening that also
158 contributes to chromosomal instability [31, 36-38]. Therefore, we analyzed the telomere
159 length of 2i-ESCs and AX-ESCs over passages. The telomere length of 2i-ESCs was
160 shorter than that of AX-ESCs (**Fig. 1j, Extended data Fig.2f**), since the telomere length
161 of AX-ESCs was maintained while that of 2i-ESCs became incrementally shortened
162 from passage 0 to 6 (**Extended data Fig. 2g).** Additionally, Zscan4, a DNA-binding
163 protein that functions for telomere elongation and maintenance in ESCs [39, 40], was
164 expressed at significantly lower levels in 2i-ESCs compared to AX-ESCs (**Fig.1k,**
165 **Extended data Fig. 2h**). Western blotting assays confirmed the Zscan4 protein was
166 present in ESCs cultured in 2iLA but missing in 2iL (**Fig.1l**). The Zscan4-GFP and
167 MERVL-tdTomato double reporter ESC line [41], was used to detect ESC transiently
168 expressed early-embryonic transcripts, *Zscan4c* [39] and *MERVL* endogenous
169 retrovirus [42]. This demonstrated that AX-ESCs exhibit a higher percentage of the
170 Zscan4 positive or Zscan4/MERVL double positive cells (**Extended data Fig. 2i)**. Thus,
171 suppression of Zscan4 expression in 2iL medium may account for the telomere
172 shortening over multiple passages, and AX supplementation alleviates this suppression,
173 thereby preventing telomere shortening during ESC *in vitro* culture.

174 **AX induces the transition of ESCs from naïve to formative-like pluripotency**

175 While AX-ESCs retained the potential to generate all-ESC mice (**Fig. 1c)**, we
176 observed that colonies of these ESCs no longer maintained the typical uniform and
177 rounded naïve colony morphology. Analyses of the core pluripotency genes, Pou5f1

178 (Oct3/4) and Sox2 by immunostaining, qPCR and western blotting assays revealed that
179 these genes are expressed at similar levels independent of culture medium (**Fig. 2a-2b**,
180 **Extended data Fig. 3a).** However, genes considered as naïve markers, such as
181 Nanog, Rex1 (Zfp42), Klf2, Klf4, Prdm14, Stat3, Essrb, and Nr0b1 are all expressed at
182 lower levels in AX-ESCs, more similar to ESCs in serum/LIF medium (**Fig. 2a-2c and**
183 **Extended data Fig. 3a)**, indicating that AX-ESCs have lost naïve stem cell gene
184 signatures and likely exited from the naïve pluripotent state. Since AX-ESCs can
185 contribute to germline and maintain the potential to generate all-ESC mice by tetraploid
186 complementation (**Fig. 1c)**, they are not yet transformed to a primed state, but are likely
187 maintained in a distinct naïve-to-primed intermediate state of pluripotency.

188 Formative pluripotency was recently proposed to describe an intermediate
189 executive phase between the naïve and primed states [9-12, 21]. This phase of
190 pluripotency is thought to be responsive to inductive cues for lineage differentiation and
191 to express a group of unique formative genes [11, 43]. We performed RNA-seq of 2i-
192 ESCs and AX-ESCs, finding 1637 genes that were differentially expressed and which
193 are significantly enriched in pluripotency genes and the MAPK signaling pathway
194 (**Extended data Fig. 3c).** Among these genes, 978 genes were upregulated in AX-
195 ESCs, including most formative genes (**Fig. 2d**)**.** Expression levels of formative genes
196 such as Wnt8a, Pou3f1, Pim2, Sall2, Sox3, c-Myc, Eras, and Lef1, were all significantly
197 higher in AX-ESCs, but silenced or expressed at low levels in 2i-ESCs (**Fig. 2b, 2d and**
198 **Extended data Fig. 3b)**. Notably, genes expressed exclusively in primed stem cells*,*
199 were not expressed in either 2i-ESCs or AX-ESCs (**Extended data Fig. 3d**).

200 Global increase of DNA methylation is anticipated in formative stem cells [11].
201 Expression levels for Dnmt3a, Dnmt3b and Dnmt3l are all higher in AX-ESCs compared
202 to ESCs cultured otherwise, both in transcripts (**Extended data Fig.3b**) and protein
203 (**Fig. 2e**). In agreement with these results, compared to the reduced total 5-
204 methylcytosine (5mC) in 2iL ESCs, AX-ESCs exhibit a significant increase similar to
205 levels seen with serum/LIF ESCs (**Fig. 2f**). Reduced-representation bisulfite sequencing
206 (RRBS-Seq) confirmed the increase of global DNA methylation at promoters (**Fig. 2g**)
207 and CpGs (**Fig. 2h**) in AX-ESCs. Of 5951 differentially methylated promoters, 5937
208 were hyper-methylated in AX-ESCs (>99%).
209 Responsiveness to inductive cues for lineage specification is another prominent
210 feature that distinguishes naïve and formative stem cells [11]. To measure
211 responsiveness, we adopted a standard directed differentiation protocol. ESCs were
212 cultured in serum free differentiation (SFD) medium to form embryoid bodies (EBs), and
213 Activin A was added at either day 0, day 1 or day 2 to induce differentiation toward
214 mesendoderm, identified by Brachyury (T) expression (**Fig. 2i**). T positive cells were
215 analyzed by flow cytometry to determine the differentiation efficiency. As expected, 2i-
216 ESCs were not responsive to stimulus in the Day 0 group, failing to generate T positive
217 cells (<0.1%) at the 4 timepoints (12h, 24h, 36h ,48h post Activin A induction) (**Fig. 2j**).
218 Intriguingly, AX-ESCs were responsive to Activin A induction though not at high
219 efficiency; approximately 5% T positive cells were found at 48h post induction (**Fig. 2j**).
220 Notably, differentiation efficiency was remarkably increased for AX-ESCs when induced
221 at Day 1 (after 24 hours in SFD medium), generating over 40% T positive cells at 36-
222 48h post induction (**Fig. 2j**), whereas induction of the 2i-ESCs remained inefficient

223 (~5%) (**Fig. 2j**). The differentiation efficiency for 2i-ESCs significantly increased and
224 reached comparable levels of AX-ESCs only when induced at Day2 (**Fig. 2j**), both
225 showing similar differentiation kinetics and producing over 20% T positive cells 42h after
226 induction (**Fig.2j**). These results are consistent with AX-ESCs acquiring a formative
227 pluripotent state that ensures relatively rapid response to inductive cues and execution
228 of lineage fate decisions. Taken together, the results indicate that AX-ESCs lose naïve
229 stem cell identity and acquire a new formative-like intermediate state of pluripotency.

230 **Lipids in AX drive pluripotency transition**

231 Previous studies of human pluripotent stem cells demonstrated that lipids in AX, not
232 albumin (BSA), support self-renewal and facilitate pluripotent cell transitions [2, 4]. To
233 test whether lipids are essential in the murine system, we first deproteinized AX (dep-
234 AX) in a manner that can efficiently remove proteins including albumin from AX, as
235 previously described [2]. ESCs cultured in 2iL medium supplemented with dep-AX
236 retained a formative colony morphology (**Fig. 3a**), while ESCs cultured in 2iL
237 supplemented with fatty acid free BSA (BSA) maintained a naïve colony morphology
238 (**Fig.3a**). Addition of chemical defined lipid components (CDLC) plus BSA in 2iL
239 medium, specifically Lipid Mixture 1 which contains non-animal derived fatty acids
240 (arachidonic, linoleic, linolenic, myristic, oleic, palmitic, stearic, cholesterol, tocopherol
241 acetate and Pluronic) could also induce the change of colony morphology (although not
242 as dramatic as with AX), clearly distinct from naïve colony morphology, being flatter and
243 much more irregularly shaped (**Fig. 3a**). Therefore, lipids, not albumin, induce the
244 change of colony morphology for murine ESCs cultured in 2iLA medium.

245 We next analyzed the impact of lipid supplementation on expression of pluripotency
246 genes. Western blot analysis showed that the protein levels of formative genes Eras, c-
247 Myc, Dnmt3a, and Dnmt3L were increased (**Fig. 3b**) while those of naïve genes Esrrb,
248 Klf2, and Klf4 were decreased in 2iL medium supplemented with AX or the saturated
249 fatty acid palmitate (**Fig. 3c**); supplementing only BSA in 2iL medium had no effect on
250 expression of these genes (**Fig. 3b, 3c**). qPCR assays demonstrated that levels of the
251 formative genes *Dnmt3s* and *Lef1* were enhanced in 2iL medium supplemented with
252 CDLC or free fatty acids (FFA) (**Fig. 3d)**. Therefore, lipids induce the expression of
253 formative genes and decrease expression of naïve genes, indicating that lipids are
254 sufficient, independent of BSA, to induce the pluripotency transition to formative-like
255 cells in 2iLA medium.

256 **Lipids in AX impact intracellular metabolism and enhanced non-canonical TCA**
257 **cycle metabolism**

258 In addition to increased steady-state levels of nucleotide pools, LC-MS analysis also
259 showed that treatment with AX enhanced the steady-state levels of the non-canonical
260 TCA cycle metabolites citrate and cis-aconitic acid (**Extended data Fig. 4a, b**), which
261 were recently reported to be engaged in the exit of naïve pluripotency [44]. qRT-PCR
262 analysis of TCA cycle enzymes showed that AX treatment did not alter expression of
263 most genes with the exception of succinate dehydrogenase (*SDHB*), which was
264 upregulated after just 24-hour treatment and sustained through passage 3 (**Extended**
265 **data Fig 4c**). In serum-free 2iL medium cells must expend high levels of reducing
266 equivalents in the form of NADPH to synthesize lipids de novo. Consistent with high
267 levels of de novo lipogenesis, ACLY, FASN, SCD1, SCD2 protein levels are increased

268 in 2iL while treatment with AX induced a strong downregulation indicating a reduction in
269 capacity for lipid biosynthetic reactions (**Extended Fig 4d-e**). Moreover, two metabolic
270 intermediates associated with lipid metabolism, glycerol-3-phosphate and
271 phosphoethanolamine, were also reduced in AX treated cells (**Extended data Fig 4f**).
272 LC-MS also revealed a steady state reduction in amino acid abundance (**Extended**
273 **data Fig 4g**), potentially a result of increased anabolic reactions and protein synthesis
274 in AX-ESCs expressing high levels of c-Myc and ERas.

275 **Lipids in AX promote genomic stability and maintain two active X chromosomes**
276 **in female ESCs**

277 We next evaluated the effect of lipids on genomic stability. Male ESCs expanded
278 under 2iL (unsupplemented), AX, dep-AX or CDLC conditions were karyotyped at P12.
279 As expected, the XY ESCs cultured in 2iL medium became aneuploid (95%), while 40%
280 of cells in 2iLA medium maintained a normal karyotype (**Fig.3e**). Medium supplemented
281 with CDLC or dep-AX promoted retention of normal ESC karyotype (60% and 70%,
282 respectively) (**Fig. 3e**). These results demonstrated that both CDLC and dep-AX can
283 significantly promote the karyotypic stability of male ESCs comparable to AX
284 supplementation of 2iL medium.

285 To investigate the effect of lipids on X chromosome loss in female ESCs, we
286 adopted the $X^{G}X^{T}$ double reporter system to monitor X chromosome loss during *in vitro*
287 culture (**Fig. 1f**). The GFP and Tomato double positive cells were sorted at passage 2 in
288 2iL and expanded in 2iL for 2 passages. The cells were then split at the same density
289 into 2iL medium alone, or supplemented with AX, dep-AX or CDLC (denoted as
290 passage 0, P0), followed by FACS analyses to assess X chromosome loss over the

291 course of *in vitro* expansion (**Fig. 3f**). The double positive cell population was
292 incrementally depleted from P1 to P15 in 2iL medium, but it was maintained at a high
293 percentage (over 95%) in 2iLA medium (**Fig. 3g**). Notably, both dep-AX and CDLC
294 supplementation also preserved a high double positive cell population (over 95%) (**Fig.**
295 **3g**), showing that lipids efficiently prevent X chromosome loss in supplemented 2iL
296 medium. Therefore, lipids can mitigate aneuploidy and stabilize the genome of murine
297 ESCs cultured in 2iL medium, supporting the notion that lipids are responsible for the
298 effects of AX on genomic stability.

299 **Lipid-induced formative-like pluripotency is maintained in concert with 2i**

300 To explore how AX interacts with the two inhibitors (2i) to induce pluripotency
301 transition and maintain genomic stability, we removed PD, CHIR or both from 2iLA
302 medium (designated as CLA, PLA or LA). Withdrawal of either or both inhibitors from
303 2iL or 2iLA media led to loss of a typical formative colony morphology as seen in 2iLA
304 (**Fig. 4a, Extended data Fig.5a**). However, LA medium supported proliferation and
305 long-term maintenance of ESCs, while with only LIF in the basic media without AX
306 massive cell death occurred during the first several passages (**Fig. 4a**). Expression
307 levels of the formative marker genes *Dnmt3b*, *Lef1* and*Pou3f1* were significantly
308 changed compared to AX-ESCs (**Extended data Fig. 5b**). The growth curve showed
309 CLA, or PLA ESC number were significantly decreased, possible because of the cell
310 death increase of the differentiated ESCs (**Fig. 4a-b**). Moreover, LA-ESCs responded
311 more rapidly to Activin A stimulus than naïve 2i-ESCs, even faster than AX-ESCs
312 (**Fig.4c**). Therefore, LA-ESCs lose naïve stem cell identity and transition to a
313 pluripotency state similar to AX-ESCs.

314 The developmental potential of LA-ESCs was assessed using tetraploid
315 complementation. Live pups were obtained from the LA-ESCs when used at early
316 passage (P3) in one cell line (ESC-1). However, this was very inefficient compared to
317 using AX-ESCs, with 4n competence completely lost by passage 10 (**Fig. 4d**). Indeed, a
318 second cell line failed to generate live pups even at early passages (P3-P6) (**Fig. 4d**).
319 Karyotyping analyses of LA cultured ESCs revealed that the genome is stable - over
320 90% of cells maintained normal karyotype at P15 (**Fig. 4e**), suggesting that the loss of
321 4n competence in LA-ESCs is due to epigenetic changes rather than genetic
322 deterioration. Therefore, ESCs cultured in LA medium maintain formative-like colony
323 morphology and express formative-like marker genes, yet do not have the full potency
324 as seen with ESCs cultured in 2iLA medium. This suggests that the formative
325 pluripotency induced by lipids in 2iLA medium is maintained in concert with the two
326 inhibitors of Mek/Erk and GSK3β signaling pathways. Notably, karyotypic analyses
327 showed that addition of either PD or CHIR promotes abnormal karyotypes in 2iL
328 medium, (especially PD). However, AX can blunt the adverse effects of PD and/or CHIR
329 on genomic stability. Most of the L-ESCs or LA-ESCs maintained karyotype stability
330 (**Fig. 4e, Extended data Fig.5c**). Additionally, AX supplement enhanced the Zscan4-
331 GFP positive population (**Fig. 4f**) in Zscan4-GFP and MERVL-tdTomato double reporter
332 ESCs (**Extended data Fig. 2i**) regardless of the inhibitors. The data indicate that the
333 ability of lipids to increase ZSCAN4 expression levels and maintain genomic stability is
334 independent of GSK3 and Erk signaling.

335 **Fatty acid oxidation (FAO) is dispensable for lipid-induced pluripotency transition**

336 To determine whether lipids or lipid metabolism (lipid metabolites) drive
337 pluripotency transition, we inhibited carnitine palmitoyltransferase (CPT1) with Etomoxir
338 (ETO) (**Extended data Fig. 6a**), an irreversible inhibitor of CPT1 on the inner face of
339 the outer mitochondrial membrane [45]. Pluripotency transition from naïve to formative
340 state was observed in ESCs cultured in 2iLA medium supplemented with ETO
341 (**Extended data Fig. 6b, 6c).** ACAA2 catalyzes the last step of the mitochondrial fatty
342 acid beta oxidation spiral (**Extended data Fig. 6a**); inhibition of ACCA2 with
343 Trimetazidine (TMZ) [46] also did not block the pluripotency transition in 2iLA medium
344 (**Extended data Fig. 6b)**. To validate these results, we took a genetic approach by
345 disruption in ESCs of the *Cpt1a* gene using CRISPR/Cas9 (**Extended data Fig. 6d)**.
346 Consistent with inhibitor results, the *Cpt1a* null ESCs displayed a formative-like colony
347 morphology in 2iLA medium (**Extended data Fig. 6e)** and increased expression levels
348 of formative gene *Dnmt3b*, based on qRT-PCR (**Extended data Fig. 6f)**. Therefore,
349 fatty acid oxidation is dispensable for the lipid-induced formative pluripotency,
350 suggesting that lipids, rather than lipid metabolism, drive pluripotency transition.

351 **Lipids drive pluripotency transition via stimulating Mek-mediated Erk2**
352 **phosphorylation**

353 While Mek/Erk signaling is thought to be inhibited by PD in 2iLA medium, western
354 blotting assays indicated that phosphorylated-Erk1/2 (p-Erk1/2) was significantly
355 increased in ESCs cultured in 2iLA medium compared to serum/LIF+2i medium (**Fig.**
356 **5a**). This suggests that AX blunts the effect of PD on the inhibition of MAPK signaling.
357 The kinetics of AX and p-Erk1/2 signaling was explored by performing a time course
358 experiment focused on genes that are upstream of Erk1/2. Mek1/2, p-Mek1/2, and p-

359 Raf (Erk upstream genes), did not respond to AX addition at the protein level, while
360 levels of p-Erk1/2 increased as early as 10 min and peaked from 20 min through 5h
361 post AX supplementation (**Fig. 5b**), with higher p-Erk1/2 levels maintained in 2iLA
362 medium thereafter (**Fig. 5b**). Notably, qPCR analyses showed that expression of
363 *Dnmt3a/b/l* were not changed until 1h after AX addition (**Extended data Fig. 7a**).
364 Therefore, the increase of p-Erk1/2 precedes the upregulation of formative genes,
365 suggesting that the change of p-Erk1/2 levels is a direct response to AX addition, rather
366 than a secondary effect of pluripotency transition.

367 To investigate if Erk1/2 signaling is involved in the pluripotency transition induced
368 by lipids, we used an ESC line in which *Erk2* is constitutively deleted and *Erk1* is
369 knocked down by shRNA (designated *Erk1/2* mutant) [47]. With the *Erk1/2* mutant, both
370 Erk1 and Erk2 proteins are depleted, while Erk2 activity can be rescued by adding back
371 the *Erk2* cDNA (Erk2-Rescue, *Erk2-Res*) (**Extended data Fig. 7b),** as confirmed by the
372 expression of *Spry4*, a direct target of the Erk1/2 signaling pathway (**Extended data**
373 **Fig. 7c)**. When culturing *Erk1/2* mutant ESCs in 2iLA medium, the expression levels for
374 formative genes *Wnt8a and Lef1* were relatively unchanged compared to the 2iL
375 controls (**Extended data Fig. 7d**), suggesting that pluripotency transition is likely
376 blocked in 2iLA medium in these cells.

377 Erk1/2 signaling is essential for self-renewal and maintenance of ESCs, and double
378 knockout of *Erk1* and *Erk2* is not tolerated *in vitro* [48]. To circumvent this problem, we
379 analyzed single *Erk2* knockout, as *Erk2* is thought to be the key gene regulating
380 pluripotency transition [49, 50]. Gene expression analysis showed that *Erk2* deletion is
381 sufficient to block response to lipid induced pluripotency transition (**Extended data Fig.**

382 **7d**). Remarkably, the pluripotency transition was severely impaired in *Erk2*$^{-/-}$ ESCs
383 induced by lipids even at passage 4, as indicated by the sustained expression of naïve
384 genes such as *Nanog* and *Prdm14*, while the expression levels of formative genes
385 *Dnmt3b* and *Pim2* remained largely unchanged (**Fig. 5c**). To test if this defect is specific
386 to lipid induced transition, we induced the *Erk2*$^{-/-}$ ESC differentiation by removal of 2i
387 and LIF from the basic N2B27 culture medium (**Fig. 5d**). Under these conditions, *Erk2*$^{-/-}$
388 cells initiated differentiation and formed differentiated colonies similar to WT ESCs at
389 72h (**Fig. 5d**). qRT-PCR analyses of the *Erk2*$^{-/-}$ cells showed that the expression levels
390 of naïve genes *Prdm14* and *Zfp42* were downregulated while those for the formative
391 genes *Dnmt3b* and *Pim2* were significantly upregulated (**Fig. 5e**). However, the
392 transcriptional changes in *Erk2*$^{-/-}$ cells after switching to N2B27 medium were relatively
393 modest compared to WT cells, suggesting a delay in the pluripotency transition, as
394 previously described for multiple mutants in the Fgf/Erk pathway including *Erk1 and*
395 *Erk2* single mutants [51]. Finally, we examined the pluripotency transition induced by
396 lipids in PSCs with *a* double knockout of *Mek1/2,* the only kinases known to be
397 responsible for Erk1/2 phosphorylation in PSCs (**Extended data Figs. 7e-7f**). Analysis
398 of pErk1/2 confirmed that phosphorylation of Erk1/2 requires p-Mek1/2 in 2iLA medium
399 (**Extended data Fig. 7h**). The pluripotency transition was significantly impaired in 2iLA
400 medium as indicated by expression levels of naïve and formative markers (**Extended**
401 **data Fig. 7g**). Furthermore, when switched from 2iL to 2iLA, deletion of *Mek1/2* or *Erk2*
402 resulted in smaller colonies compared to *WT* or *Erk2-Re*s, with reduced proliferation
403 than the control, based on the colony size (**Extended data Fig. 7i**). Also, both the naive
404 gene *Nanog* and the formative gene *Dnmt3l* were deregulated after switching into 2iLA

405 (**Extended data Fig. 7j**). This result suggests that stimulation of Erk2 by lipids requires
406 Mek. Together, our results indicate that lipids can stimulate Mek-mediated Erk2
407 phosphorylation which is essential for lipid-induced pluripotency transition.

408 **Erk1/2 suppression leads to X chromosome loss in female ESCs**

409 The cause of X chromosome loss when female ESCs are cultured in 2iL is unclear,
410 although it has been suggested to be related to Wnt and Mapk signaling [28]. We
411 showed that adding lipids in 2iL medium efficiently prevents X chromosome loss (**Fig.**
412 **3g**), while p-Erk1/2 level is increased in this condition (**Fig 5a**). We hypothesized that
413 suppression of Erk1/2 signaling in 2iL medium is responsible for X chromosome loss in
414 XX ESCs, whereas lipid-induced increase of Erk1/2 signaling attenuates X chromosome
415 loss. Using the $X^{G}X^{T}$ reporter ESC line, FACS analyses showed that ESCs cultured in
416 2iL or serum/LIF/2i (SL2i) with lower p-Erk1/2 underwent significant X chromosome loss
417 by passage 15, while in 2iLA, ESCs maintained over 95% of two active X chromosomes
418 (**Fig. 5f**). To determine if Erk1/2 signaling is associated with X chromosome loss, we
419 inhibited Erk2 activity using VX-11e, a small molecule inhibitor of Erk2 [52] in 2iLA or
420 CLA medium (2iLA+VX-11e or CLA+ VX-11e). Indeed, significant X chromosome loss
421 was observed (over 30% loss of X chromosome after P9) in ESCs cultured in 2iLA+VX-
422 11e medium (**Fig. 5g**). The result supports the notion that suppression of Erk signaling
423 is associated with X chromosome loss in XX ESCs cultured in 2iL medium. Moreover,
424 genetic deletion of Mek1/2 or Erk2 in ESCs demonstrated that nearly 100% of ESCs
425 lost one X chromosome by passage 16 or 18 even when cultured in 2iLA medium (**Fig.**
426 **5h**), suggesting that Mek/Erk signaling is critical for maintenance of two X
427 chromosomes in ESCs. Collectively, our results suggest that prolonged suppression of

428 Mek/Erk signaling is responsible for the X chromosome loss in ESCs cultured in 2iL
429 medium and lipids prevent X chromosome loss through increase of p-Erk1/2.

430 **Lipid-induced formative-like pluripotency is reversible**

431 We tested if the naïve to formative pluripotent state induced by lipids could be
432 reversed upon withdrawal of lipids. Indeed, AX-ESCs that maintained stable formative
433 features for >10 passages formed typical naïve colony morphology when switched to
434 2iL medium (designated R-ESCs) (**Fig. 6a**). Bulk RNA-seq on these cells showed that
435 upon withdrawal, naïve markers were enhanced whereas formative markers were
436 decreased (**Fig. 6b**). Like 2i-ESCs, the endogenous nucleotide pools were significantly
437 depleted in R-ESCs (**Fig. 6c**). Western blotting assays confirmed that in R-ESCs,
438 expression of p-Erk1/2, Dnmt3a/b and Zscan4 decreased to levels found in naïve 2i-
439 ESCs (**Fig. 6d**). Using the *in vitro* system described above to test responsiveness to
440 differentiation stimuli (**Fig. 2i**), Activin A induction of T positive cells was decreased for
441 R-ESCs (**Fig. 6e**). Our results suggest that the formative state of AX-ESCs can revert
442 fully back to a naïve state by withdrawal of AX from the culture medium.

443 **Lipid-induced pluripotency transition is restrained through manipulation of**
444 **Fgf/Erk signaling**

445 We next asked whether the lipid-induced pluripotency transition can be restrained
446 through inhibition of p-Erk1/2 using specific Erk inhibitors to counteract the effects of
447 lipids (**Extended data Fig.8a**). The small molecule SCH772984 is a unique, selective
448 and ATP competitive inhibitor of Erk1/2 signaling that acts by inhibiting phosphorylation
449 of the Erk1/2 substrate p90 ribosomal S6 kinase [53]. SCH772984 was added to ESCs
450 previously maintained in 2iLA medium (designated 2iLA+iErk) for 3 passages. ESCs in

451 2iLA+iErk medium displayed typical naïve colony morphology (**Fig. 6a**) and the
452 proliferation rate slowed (**Extended data Fig.8c)**. Analyses of pluripotency marker
453 genes confirmed decreased levels of formative genes including *Lef1* and *Dnmt3b/l* (**Fig.**
454 **6f**). These results demonstrate that lipid-induced formative pluripotency can be reversed
455 to naïve state simply through manipulation of Erk1/2 signaling.

456 FGFR is upstream of the Erk1/2 signaling, and RNA-seq data confirmed increased
457 expression levels for many FGF/MAPK/ERK pathway related genes in 2iLA conditions
458 (**Extended data Fig.8a-8b**), including for *Fgf5* which is a validated epiblast or mEpiSC
459 marker [54, 55]. Fgf5 interacts with membrane-bound receptor Fgfr1 to activate
460 intracellular signaling cascades including PI3K-AKT, PLCγ, MAPK and STAT pathways
461 [56]. Modulating FGF signaling was proposed to manipulate pluripotency state
462 conversion [57], with inhibition of Fgfr as a means of maintaining murine ESCs in a
463 more naïve state [8]. We added an inhibitor of Fgfr1/2/3, AZD4547 [58], to 2iLA medium
464 (Designated 2iLA+iFgfr). Intriguingly, the AX-ESCs were reverted from formative to
465 naïve state by this treatment (**Fig. 6a, 6f-6g**). The *in vivo* developmental potential of
466 iErk/iFgfr-cultured ESCs was evaluated by tetraploid complementation. Both iErk and
467 iFgfr cultured ESCs generated viable and healthy all-ESC pups with high efficiency (**Fig.**
468 **6h, Extended data Fig. 8d**), demonstrating that full pluripotency was preserved in
469 these naïve ESCs that reverted from the formative state.

470 Supplementation of AX into 2iL medium significantly improves genomic stability and
471 induced transition from naïve to formative pluripotency. To understand whether these
472 phenotypes are intrinsically connected, genomic stability of ESCs cultured in 2iLA+iErk
473 or 2iLA+iFgfr media was analyzed. Notably, ESCs cultured in 2iLA medium (formative

474 pluripotency) maintained approximately 30% normal karyotypes, while ESCs cultured in
475 either iErk or iFgfr conditions, even though appearing to be in a naïve pluripotent state,
476 achieved over 40% and 20% normal karyotype cells at passage 12, respectively
477 (**Extended data Fig. 8e**). We found that *Zscan4* expression levels, highly correlated
478 with telomere length maintenance, were significantly higher in both iErk and iFgfr-ESCs
479 compared to 2i-ESCs (**Fig. 6i**), indicating that telomere length is maintained in these
480 ESCs. The results suggest that the improvement of genomic stability by lipid
481 supplementation is independent of naïve or formative pluripotency state.

482 Therefore, formative AX-ESCs can fully revert to naïve state in terms of their colony
483 morphology, transcript profile, and responsiveness to stimuli, by simply withdrawing AX
484 from the culture medium. Addition of Fgf/Erk-specific inhibitors in 2iLA medium also
485 reverts ESC cells to naïve state, retaining full pluripotency, but also with significant
486 improvement of genomic stability (**Fig. 6j**), suggesting that lipid-induced pluripotency
487 transition can be restrained through manipulating Fgf/Erk signaling.

488 **Male and female all-ESC mice are generated from de novo derived ESCs using**
489 **AX-based medium**

490 We next explored derivation of ESCs from E3.5-4.5 embryos from different strains
491 using 2iLA and assessed the developmental potential by tetraploid complementation
492 (**Fig. 7a**). After removal of the zona pellucida, E3.5-4.5 embryos were placed into a 96-
493 well plate on feeders and cells expanded in 2iLA medium (**Extended data Fig. 8f**). Male
494 and female ESC lines were derived from F1 (129X B6) using 2iLA medium. All-ESC
495 mice can be generated from both male and female cell lines to obtain live pups, with
496 24.7% and 18.5% efficiency, respectively (live pups/embryos transferred, **Fig. 7b,**

497 **Extended data Fig. 8f**). Both male and female all-ESC pups appeared normal and
498 survived to adulthood. We also derived ESCs from the inbred C57B6 strain using 2iLA
499 medium and found all-ESC pups can be generated from these, although not as
500 efficiently as with the F1 hybrid strain (**Fig. 7b**). The outbred ICR line has been
501 considered a non-permissive strain to derive ESCs [43, 59]. Using 2iLA medium, we
502 efficiently derived ICR ESC lines from E3.5-E4.5 blastocysts. Both male and female ICR
503 ESC lines generated all-ESC pups via tetraploid complementation with an efficiency of
504 6.7% for male and 12.5% for female (**Fig. 7b, Extended data Fig. 8f**). Our studies
505 demonstrated that supplementing AX into 2iL medium (2iLA) enabled derivation of both
506 male and female ESC lines with full potential to generate all-ESC pups, suggesting that
507 lipids maintain genomic stability and developmental potential during ESC derivation.
508 Our results suggested that PD0325901(PD) is a major cause of genomic instability
509 in cultured ESCs (**Fig. 4e**). To test if PD can be replaced by Erk1/2 inhibitors for ESC
510 derivation, we substituted PD with the p-Erk1/2 inhibitor SCH772984 in 2iLA medium
511 (CHIR/ SCH772984/LIF/AlbuMAX, designated CSA). ESC lines were readily generated
512 from F1, ICR, and B6 strains with an efficiency as high as with 2iLA medium (**Extended**
513 **data Fig. 8f**). The efficiency to obtain all-ESC pups were improved for the non-
514 permissive strains of ICR (XX: 10.7%, XY: 20.0%) and B6 (XX: 9.4%, XY: 11.1%), while
515 a similar efficiency as in 2iLA medium was achieved for the F1 strain (**Fig. 7c-d,**
516 **Extended data Fig. 8g**). All-ESC mice generated from both male and female ESCs (F1,
517 ICR, and B6) were normal and fertile (**Fig. 7c-7d**). Our results demonstrate that PD, the
518 Mek1/2 inhibitor, can be substituted with Erk1/2 inhibitors for ESC derivation,

519 suggesting that p-Erk1/2 direct inhibition and Wnt agonist are sufficient to preserve
520 pluripotency for ESC derivation and maintenance in AX medium.

521 **Generation of all-ESC mice from ESCs de novo derived from late-stage**
522 **blastocysts**

523 Finally, we derived ESC lines directly from late-stage embryos (E5.5) using 2iLA
524 medium and tested the cell lines for 4n competence through generation of all-ESC mice
525 (**Fig. 7a**). We obtained and cultured 23 hatching blastocysts (E5.5) in the stage of
526 embryonic escape from the zona pellucida (**Fig. 7e**). Embryos were placed individually
527 into a 96-well plate on feeders and cells expanded in 2iLA medium. The ICM outgrowths
528 emerged from all embryos at day 7 and cell lines were successfully established from
529 each embryo (**Fig. 7e**). The colony morphology of these cell lines was distinct from
530 ESCs cultured in 2iL medium and resembled the formative morphology of ESCs
531 cultured in 2iLA medium (**Fig. 7e**). Notably, colonies from female cell lines were flatter
532 and more irregular-shaped than those from male cell lines (**Fig. 7e**). The female cell
533 lines derived in 2iLA medium were karyotyped and they maintained 25-35% normal 40,
534 XX karyotypes at passage 20, while nearly all cells (over 90%) became aneuploid
535 following 12 passage culture in 2iL medium, even if they were first cultured in 2iLA for 8
536 passages (**Fig. 7f, 7g**). Therefore, both male and female ESC lines can be efficiently
537 derived from E5.5 blastocysts with improved genomic stability when maintained in 2iLA
538 medium.

539 We next evaluated the developmental potential of male and female ESC lines
540 derived from late stage blastocysts. All 4 male lines tested generated all-ESC pups with
541 efficiencies from 25% to 30% (**Fig. 7h**). The pregnant surrogates carrying these

542 embryos delivered naturally at term and the all-ESC pups were healthy and grew
543 normally to fertile adults (**Fig. 7i**). Female ESC lines generated all-ESC pups through
544 tetraploid complementation with efficiencies from 10% to 25% (**Fig. 7h**). Female all-ESC
545 pups were normal and survived to adulthood (**Fig. 7j, 7k**), producing normal litters when
546 crossed with male all-ESC mice (**Fig. 7l**). These results affirm that full pluripotency and
547 4n competence can be preserved in both male and female ESCs derived from late-
548 stage blastocysts in 2iLA medium.

549 **DISCUSSION**

550 Stabilization of pluripotency for both male and female ESCs during long-term culture
551 would benefit research into the mechanisms of cell fate determination, epigenetic
552 reprogramming, and modeling of early development using synthetic embryos. We show
553 that supplementing 2i/LIF medium with lipid-rich albumin AlbuMAX significantly
554 improves the genomic stability and developmental potential of murine ESCs. ESCs
555 cultured in 2i/LIF+AX (2iLA) medium can be propagated in a state highly similar to
556 formative pluripotency, which can be reversed to naïve pluripotency through
557 withdrawing AX or adding additional FGF/Erk-specific inhibitors. Mechanistically, lipids
558 directly stimulate Mek-mediated Erk2 phosphorylation, leading to exit of naïve state and
559 establishing formative pluripotency for ESCs cultured in 2iLA medium. Lipid metabolism
560 through β-oxidation is dispensable for transition from naïve to formative state. Lipid
561 metabolism reduces the lipogenesis and amino acid biosynthesis and promotes non-
562 canonical TCA metabolites recently reported to be involved in pluripotency transition
563 [60]. Lipid metabolism promotes nucleotide and Acyl-CoA biosynthesis, enhances the
564 expression of ZSCAN4 and DNMT3s that are involved in the maintenance of telomere

565 length and DNA methylation, thereby improving genome stability during long-term
566 culture. Stimulated Erk2 activity by lipids also alleviates X chromosome loss and
567 possibly trisomy for ESCs cultured in 2iLA medium. The dual role of lipids on genome
568 stability and pluripotency facilitates the preservation of 4n competency of murine ESCs
569 for both sexes during long-term culture in vitro (**Extended data Fig. 9**). Successful
570 generation of healthy, fertile female all-ESC mice from de novo derived ESCs
571 demonstrates that AX-based culture media support derivation of fully potent murine
572 ESCs of both sexes. Interestingly, in this AX-based system, PD, the Mek inhibitor, can
573 be substituted with an Erk inhibitor (CSA), for efficient ESC derivation from various
574 mouse strains.

575 It is known that lipids serve as signaling molecules in regulation of the Ras-Raf-Mek-
576 Erk pathway [4, 61]. Our data show that Erk1/2 rapidly senses the addition of AX to
577 elevate p-Erk1/2 independently of upstream Raf and Mek (**Fig. 5b**), and Mek1/2 is
578 essential for the phosphorylation of Erk1/2 (**Extended data Fig.7h**), indicating that lipids
579 regulating Erk2 phosphorylation might act through changing Mek1/2 kinase domain
580 conformation, which is thought to be inhibited by PD. However, whether this is an effect
581 induced by specific types of lipids needs to be further studied. While lipid-induced
582 fPSCs share common features of formative pluripotency, they are distinct from other
583 fPSCs reported in their transcriptional profiles, X chromosome inactivation, and
584 developmental potential, suggesting that fPSCs can exist in sub-states reflecting the
585 developmental continuum of pluripotency. We demonstrated that the lipid-induced
586 fPSCs retain full potency to generate “all-ESC” mice, supporting the notion that fPSCs
587 still possess unrestricted developmental potential.

588 The discovery of the 2i system [8] revolutionized both stem cell culture and
589 derivation, not only for mice but also other mammalian species including humans [23-
590 26, 62, 63]. Yet the 2i system has also been found to cause irreversible genetic and
591 epigenetic changes in murine ESCs [28, 29]. The modified 2i systems (2iLA and CSA),
592 supplemented with lipid-rich albumin, can efficiently prevent the detrimental effects of 2i
593 and preserve pluripotency while maintaining genomic stability. This improvement
594 provides a reliable culture system for targeting of ESCs and generating genetically
595 modified mice, and also for modeling developmental processes, which depend on the
596 genetic and phenotypic fidelity of ESCs during propagation. Female cells are typically
597 sensitive to 2i resulting in loss of an X chromosome and DNA methylation; thus, female
598 ESC lines derived using 2i have lost developmental potential [28, 29]. The modified
599 2iLA system can efficiently derive female cell lines that retain the potential to generate
600 fertile all-ESC mice, suggesting that the genetic and epigenetic fidelity has been
601 preserved. Therefore, the 2iLA system can be used for de novo derivation of pluripotent
602 stem cell lines including even for non-permissive strains.

603 In summary, our findings underscore the importance of lipids in cell culture media for
604 maintenance of genomic, epigenomic and phenotypic integrity, and discover novel
605 mechanisms governing pluripotent cell transitions that are conserved in early
606 mammalian development from mice to humans.

607

608

609

610 **Data availability**

611 The all the RNA-seq and RRBS data have been uploaded to the NBCI BioProject. The
612 accession number is uploaded to the Gene Expression Omnibus website. The
613 accession number is PRJNA806916.

614 **Acknowledgements**

615 We thank Dr. Fuqian Geng for the help with western blots. We would like to thank the
616 Epigenomics Core Facility and Genomic Resource Co-facility at Weill Cornell Medicine
617 for RRBS-seq, ChIP-seq and RNA-seq, and the Metabolomics & Lipidomics facility at
618 The Rockefeller University for Liquid chromatography–mass spectrometry. This work
619 was supported by the New York State Stem Cell Science Program (NYSTEM; contract
620 C32581GG to D.W.), grant no. R01 GM129380-01 and 1 R21 OD031973-01 from the
621 National Institutes of Health (to D.W.).

622 **Author contributions**

623 D.W., B.C. and T.E. conceived the project and D.W., L.Z., B.C. and T.E. wrote the
624 paper. M.G. and L.Z. performed the in vitro differentiation experiments. D.W. performed
625 the blastocyst injection and tetraploid complementation assay. Y.Q. and D.W. derived
626 the ESC lines from blastocysts. L.Z. performed the in vitro cell-culture, FACS, real-time
627 PCR, library preparation for RNA-seq, RRBS-seq and metabolic profiling. B.C. and A.S.
628 performed the metabolic profiling, western blot, immunostaining, FACS, and real-time
629 PCR. G.N. and L.Z. performed karyotyping. X.W. and Y.H. contributed to the
630 bioinformatics analysis, D.J., R.K. and C.D.A. offered insightful discussions, helped
631 interpret the results and edited the manuscript.

632 **DECLARATION OF INTERESTS**

633 A patent application has been submitted by Weill Cornell Medicine at Cornell University

634 based on these results.

635 **References:**

636 1. Tsogtbaatar, E., et al., *Energy Metabolism Regulates Stem Cell Pluripotency.*
637 Frontiers in Cell and Developmental Biology, 2020. **8**.
638 2. Cornacchia, D., et al., *Lipid Deprivation Induces a Stable, Naive-to-Primed*
639 *Intermediate State of Pluripotency in Human PSCs.* Cell Stem Cell, 2019. **25**(1):
640 p. 120-136 e10.
641 3. Xu, F., et al., *Lysophosphatidic acid shifts metabolic and transcriptional*
642 *landscapes to induce a distinct cellular state in human pluripotent stem cells.* Cell
643 Rep, 2021. **37**(9): p. 110063.
644 4. Garcia-Gonzalo, F.R. and J.C.I. Belmonte, *Albumin-Associated Lipids Regulate*
645 *Human Embryonic Stem Cell Self-Renewal.* Plos One, 2008. **3**(1).
646 5. Evans, M.J. and M.H. Kaufman, *Establishment in Culture of Pluripotential Cells*
647 *from Mouse Embryos.* Nature, 1981. **292**(5819): p. 154-156.
648 6. Martin, G.R., *Isolation of a Pluripotent Cell-Line from Early Mouse Embryos*
649 *Cultured in Medium Conditioned by Teratocarcinoma Stem-Cells.* Proceedings of
650 the National Academy of Sciences of the United States of America-Biological
651 Sciences, 1981. **78**(12): p. 7634-7638.
652 7. Hackett, J.A. and M.A. Surani, *Regulatory Principles of Pluripotency: From the*
653 *Ground State Up.* Cell Stem Cell, 2014. **15**(4): p. 416-430.
654 8. Ying, Q.L., et al., *The ground state of embryonic stem cell self-renewal.* Nature,
655 2008. **453**(7194): p. 519-U5.
656 9. Kinoshita, M., et al., *Capture of Mouse and Human Stem Cells with Features of*
657 *Formative Pluripotency.* Cell Stem Cell, 2021. **28**(3): p. 453-+.

658 10. Neagu, A., et al., *In vitro capture and characterization of embryonic rosette-stage*
659 *pluripotency between naive and primed states.* Nature Cell Biology, 2020. **22**(5).
660 11. Smith, A., *Formative pluripotency: the executive phase in a developmental*
661 *continuum.* Development, 2017. **144**(3): p. 365-373.
662 12. Wang, X.X., et al., *Formative pluripotent stem cells show features of epiblast*
663 *cells poised for gastrulation.* Cell Research, 2021.
664 13. Tesar, P.J., et al., *New cell lines from mouse epiblast share defining features*
665 *with human embryonic stem cells.* Nature, 2007. **448**(7150): p. 196-U10.
666 14. Brons, I.G.M., et al., *Derivation of pluripotent epiblast stem cells from mammalian*
667 *embryos.* Nature, 2007. **448**(7150): p. 191-U7.
668 15. Wen, D., et al., *Completely ES cell-derived mice produced by tetraploid*
669 *complementation using inner cell mass (ICM) deficient blastocysts.* PLoS One,
670 2014. **9**(4): p. e94730.
671 16. George, S.H.L., et al., *Developmental and adult phenotyping directly from mutant*
672 *embryonic stem cells.* Proceedings of the National Academy of Sciences of the
673 United States of America, 2007. **104**(11): p. 4455-4460.
674 17. Eggan, K., et al., *Hybrid vigor, fetal overgrowth, and viability of mice derived by*
675 *nuclear cloning and tetraploid embryo complementation.* Proceedings of the
676 National Academy of Sciences of the United States of America, 2001. **98**(11): p.
677 6209-6214.
678 18. Nagy, A., et al., *Derivation of Completely Cell Culture-Derived Mice from Early-*
679 *Passage Embryonic Stem-Cells.* Proceedings of the National Academy of
680 Sciences of the United States of America, 1993. **90**(18): p. 8424-8428.

681 19. Huang, Y.L., et al., *In Vivo Differentiation Potential of Epiblast Stem Cells*
682 *Revealed by Chimeric Embryo Formation.* Cell Reports, 2012. **2**(6): p. 1571-
683 1578.
684 20. Yang, P.Y., et al., *Multi-omic Profiling Reveals Dynamics of the Phased*
685 *Progression of Pluripotency.* Cell Systems, 2019. **8**(5): p. 427-+.
686 21. Yu, L.Q., et al., *Derivation of Intermediate Pluripotent Stem Cells Amenable to*
687 *Primordial Germ Cell Specification.* Cell Stem Cell, 2021. **28**(3): p. 550-+.
688 22. Wang, X.X., et al., *Formative pluripotent stem cells show features of epiblast*
689 *cells poised for gastrulation.* Cell Research, 2021. **31**(5): p. 526-541.
690 23. Li, P., et al., *Germline Competent Embryonic Stem Cells Derived from Rat*
691 *Blastocysts.* Cell, 2008. **135**(7): p. 1299-1310.
692 24. Buehr, M., et al., *Capture of Authentic Embryonic Stem Cells from Rat*
693 *Blastocysts.* Cell, 2008. **135**(7): p. 1287-1298.
694 25. Czechanski, A., et al., *Derivation and characterization of mouse embryonic stem*
695 *cells from permissive and nonpermissive strains.* Nature Protocols, 2014. **9**(3): p.
696 559-574.
697 26. Guo, G., et al., *Naive Pluripotent Stem Cells Derived Directly from Isolated Cells*
698 *of the Human Inner Cell Mass.* Stem Cell Reports, 2016. **6**(4): p. 437-446.
699 27. Mulas, C., et al., *Defined conditions for propagation and manipulation of mouse*
700 *embryonic stem cells (vol 146, dev173146, 2019).* Development, 2019. **146**(7).
701 28. Choi, J., et al., *Prolonged Mek1/2 suppression impairs the developmental*
702 *potential of embryonic stem cells.* Nature, 2017. **548**(7666): p. 219-223.

703 29. Yagi, M., et al., *Derivation of ground-state female ES cells maintaining gamete-*
704 *derived DNA methylation.* Nature, 2017. **548**(7666): p. 224-227.
705 30. Yuan, L., et al., *Female germ cell aneuploidy and embryo death in mice lacking*
706 *the meiosis-specific protein SCP3.* Science, 2002. **296**(5570): p. 1115-1118.
707 31. Pai, C.C. and S.E. Kearsey, *A Critical Balance: dNTPs and the Maintenance of*
708 *Genome Stability.* Genes, 2017. **8**(2).
709 32. Magdalou, I., et al., *The causes of replication stress and their consequences on*
710 *genome stability and cell fate.* Seminars in Cell & Developmental Biology, 2014.
711 **30**: p. 154-164.
712 33. Fasullo, M. and L. Endres, *Nucleotide Salvage Deficiencies, DNA Damage and*
713 *Neurodegeneration.* International Journal of Molecular Sciences, 2015. **16**(5): p.
714 9431-9449.
715 34. Visentin, L.P., et al., *Ribosomal-Protein S1-S1a in Bacteria.* Febs Letters, 1977.
716 **79**(2): p. 258-263.
717 35. Li, S., et al., *Crystal structure of human phosphoribosylpyrophosphate*
718 *synthetase 1 reveals a novel allosteric site.* Biochemical Journal, 2007. **401**: p.
719 39-47.
720 36. Gupta, A., et al., *Telomere Length Homeostasis Responds to Changes in*
721 *Intracellular dNTP Pools.* Genetics, 2013. **193**(4): p. 1095-+.
722 37. Maciejowski, J. and T. de Lange, *Telomeres in cancer: tumour suppression and*
723 *genome instability (vol 18, pg 175, 2017).* Nature Reviews Molecular Cell
724 Biology, 2019. **20**(4): p. 259-259.

725 38. Brind'Amour, J., et al., *An ultra-low-input native ChIP-seq protocol for genome-*
726 *wide profiling of rare cell populations.* Nat Commun, 2015. **6**: p. 6033.
727 39. Zalzman, M., et al., *Zscan4 regulates telomere elongation and genomic stability*
728 *in ES cells.* Nature, 2010. **464**(7290): p. 858-U66.
729 40. Nakai-Futatsugi, Y. and H. Niwa, *Zscan4 Is Activated after Telomere Shortening*
730 *in Mouse Embryonic Stem Cells.* Stem Cell Reports, 2016. **6**(4): p. 483-495.
731 41. Yang, F., et al., *DUX-miR-344-ZMYM2-Mediated Activation of MERVL LTRs*
732 *Induces a Totipotent 2C-like State.* Cell Stem Cell, 2020. **26**(2): p. 234-250 e7.
733 42. Macfarlan, T.S., et al., *Embryonic stem cell potency fluctuates with endogenous*
734 *retrovirus activity.* Nature, 2012. **487**(7405): p. 57-63.
735 43. Han, N.R., et al., *Generation of embryonic stem cells derived from the inner cell*
736 *mass of blastocysts of outbred ICR mice.* Animal Cells and Systems, 2020.
737 **24**(2): p. 91-98.
738 44. Arnold, P.K., et al., *A non-canonical tricarboxylic acid cycle underlies cellular*
739 *identity.* Nature, 2022. **603**(7901): p. 477-481.
740 45. Kruszynska, Y.T. and H.S.A. Sherratt, *Glucose Kinetics during Acute and*
741 *Chronic Treatment of Rats with 2[6(4-Chlorophenoxy)Hexyl]Oxirane-2-*
742 *Carboxylate, Etomoxir.* Biochemical Pharmacology, 1987. **36**(22): p. 3917-3921.
743 46. Kantor, P.F., et al., *The antianginal drug trimetazidine shifts cardiac energy*
744 *metabolism from fatty acid oxidation to glucose oxidation by inhibiting*
745 *mitochondrial long-chain 3-ketoacyl coenzyme A thiolase.* Circulation Research,
746 2000. **86**(5): p. 580-588.

747 47. Tee, W.W., et al., *Erk1/2 Activity Promotes Chromatin Features and RNAPII*
748 *Phosphorylation at Developmental Promoters in Mouse ESCs.* Cell, 2014.
749 **156**(4): p. 678-690.
750 48. Chen, H.X., et al., *Erk signaling is indispensable for genomic stability and self-*
751 *renewal of mouse embryonic stem cells.* Proceedings of the National Academy of
752 Sciences of the United States of America, 2015. **112**(44): p. E5936-E5943.
753 49. Kunath, T., et al., *FGF stimulation of the Erk1/2 signalling cascade triggers*
754 *transition of pluripotent embryonic stem cells from self-renewal to lineage*
755 *commitment.* Development, 2007. **134**(16): p. 2895-2902.
756 50. Hamilton, W.B. and J.M. Brickman, *Erk Signaling Suppresses Embryonic Stem*
757 *Cell Self-Renewal to Specify Endoderm.* Cell Reports, 2014. **9**(6): p. 2056-2070.
758 51. Leeb, M., et al., *Genetic Exploration of the Exit from Self-Renewal Using Haploid*
759 *Embryonic Stem Cells.* Cell Stem Cell, 2014. **14**(3): p. 385-393.
760 52. Aronov, A.M., et al., *Structure-Guided Design of Potent and Selective*
761 *Pyrimidylpyrrole Inhibitors of Extracellular Signal-Regulated Kinase (ERK) Using*
762 *Conformational Control.* Journal of Medicinal Chemistry, 2009. **52**(20): p. 6362-
763 6368.
764 53. Morris, E.J., et al., *Discovery of a Novel ERK Inhibitor with Activity in Models of*
765 *Acquired Resistance to BRAF and MEK Inhibitors.* Cancer Discovery, 2013. **3**(7):
766 p. 742-750.
767 54. Mossahebi-Mohammadi, M., et al., *FGF Signaling Pathway: A Key Regulator of*
768 *Stem Cell Pluripotency.* Frontiers in Cell and Developmental Biology, 2020. **8**.

769 55. Nichols, J. and A. Smith, *Naive and Primed Pluripotent States.* Cell Stem Cell,
770 2009. **4**(6): p. 487-492.
771 56. Ornitz, D.M. and N. Itoh, *The Fibroblast Growth Factor signaling pathway.* Wiley
772 Interdiscip Rev Dev Biol, 2015. **4**(3): p. 215-66.
773 57. Lanner, F. and J. Rossant, *The role of FGF/Erk signaling in pluripotent cells.*
774 Development, 2010. **137**(20): p. 3351-3360.
775 58. Gavine, P.R., et al., *AZD4547: An Orally Bioavailable, Potent, and Selective*
776 *Inhibitor of the Fibroblast Growth Factor Receptor Tyrosine Kinase Family.*
777 Cancer Research, 2012. **72**(8): p. 2045-2056.
778 59. Lee, K.H., et al., *Simple and Efficient Derivation of Mouse Embryonic Stem Cell*
779 *Lines Using Differentiation Inhibitors or Proliferation Stimulators.* Stem Cells and
780 Development, 2012. **21**(3): p. 373-383.
781 60. Arnold, P.K., et al., *A non-canonical tricarboxylic acid cycle underlies cellular*
782 *identity.* Nature, 2022. **603**(7901): p. 477-+.
783 61. Anderson, D.H., *Role of lipids in the MAPK signaling pathway.* Progress in Lipid
784 Research, 2006. **45**(2): p. 102-119.
785 62. Van der Jeught, M., et al., *Application Of Small Molecules Favoring Naive*
786 *Pluripotency during Human Embryonic Stem Cell Derivation.* Cellular
787 Reprogramming, 2015. **17**(3): p. 170-180.
788 63. Ware, C.B., et al., *Derivation of naive human embryonic stem cells.* Proceedings
789 of the National Academy of Sciences of the United States of America, 2014.
790 **111**(12): p. 4484-4489.

791 64. Gu, H., et al., *Preparation of reduced representation bisulfite sequencing libraries*
792 *for genome-scale DNA methylation profiling.* Nat Protoc, 2011. **6**(4): p. 468-81.
793 65. Akalin, A., et al., *Base-pair resolution DNA methylation sequencing reveals*
794 *profoundly divergent epigenetic landscapes in acute myeloid leukemia.* PLoS
795 Genet, 2012. **8**(6): p. e1002781.
796 66. Dodt, M., et al., *FLEXBAR-Flexible Barcode and Adapter Processing for Next-*
797 *Generation Sequencing Platforms.* Biology (Basel), 2012. **1**(3): p. 895-905.
798 67. Krueger, F. and S.R. Andrews, *Bismark: a flexible aligner and methylation caller*
799 *for Bisulfite-Seq applications.* Bioinformatics, 2011. **27**(11): p. 1571-2.
800 68. Langmead, B. and S.L. Salzberg, *Fast gapped-read alignment with Bowtie 2.* Nat
801 Methods, 2012. **9**(4): p. 357-9.

802 **FIGURE LEGENDS:**

803 **Fig.1|AX improves developmental potential and genomic stability of murine ESCs.**
804 **a,** Schematic illustration of the experimental design. **b,** Colony morphology for ESCs
805 cultured in 2iL or 2iLA at passage 3 or passage 15. Scale, 25 μm. **c,** Developmental
806 potential assessed by tetraploid complementation. The numbers at each timepoint
807 represent total No. pups/No.embryos transferred. **d-e,** Analysis for normal karyotype (**d**)
808 in 2iL and 2iLA at different passages (n=~20 metaphases at each passage for 2iL or
809 2iLA). Representative severe chromosome loss (**e**) in 2iL at P43. Arrow: Chromosome
810 loss. **f,** FACS analysis of XGXT reporter female ESC cultured in 2iL or 2iLA. The double
811 reporter positive cells indicate both X chromosomes are maintained. **g,** Karyotyping of
812 the XGXT ESCs cultured in 2iL and 2iLA at passage 15. **h,** LC-MS analysis of
813 nucleotide pools for ESCs cultured in 2iL and 2iLA (P3). **i,** Prps2 expression levels by
814 qRT-PCR assay or Western blot assay. **P<0.01, ***P<0.001, t-test. **j,** the telomere
815 length analyzed by qRT-PCR relative to a single copy gene (T/S) for ESCs cultured in
816 2iL or 2iLA at different passages. * P<0.05, **P<0.01, t-test. **k-l,** Relative Zscan4
817 transcript (**k**) or protein (**l**) levels by qRT-PCR analysis or Western blot assay.
818 ****P<0.0001, t-test.

819 **Fig.2 | AX induces the transition of ESCs from naive to formative-like**
820 **pluripotency. a,** Immunostaining for Oct4 (red) and Nanog (green) of ESCs cultured in
821 2il or 2iLA. DAPI (Blue) for cell nuclei. **b,** Western blotting of the naive,formative or
822 general pluripotency marker protein level in SL,SL2i,2iL or 2iLA. **c,** FACS analysis using
823 a GFP:Nanog ESC reporter line, the GFP fluorescence intensity is decreased in 2iLA. **d,**
824 Heatmap of transcript levels from bulk RNA-seq for the naive and formative genes

825 cultured in 2iL or 2iLA at P3. Three different ESC lines for biological replicates. **e,**
826 Dnmt3a/b levels demonstrated by western blotting assays. **f,** LC-MS showing the global
827 levels of 5mC/C ratio in genomic DNA from ESCs cultured in different media. **g,** Violin
828 plots of the DNA methylation distribution rate at promoter regions in ESCs cultured in
829 2iL or 2iLA at P3 from reduced representation bisulfite sequencing (RRBS). Three
830 biological replicates. **h,** RRBS for quantification of the average global methylation rate in
831 all CpGs. Three biological replicates. **i,** Schematic of the assay to test responsiveness
832 to Activin A for differentiation. **j,** FACS analysis of the mesendoderm differentiation
833 marker brachyury (T) positive cells at different time points after Activin A (AcA) addition
834 at Day0 (D0), Day1 (D1) or Day2 (D2) embryoid body formation. D0, D2 two biological
835 replicates, D1 three biological replicates.

836 **Fig.3 | Lipids in AX drive the pluripotency transition and promote genomic**
837 **stability. a,** Colony morphology is shown for ESCs cultured in 2iL, 2iL+BSA (0.1%fatty
838 acid free BSA), 2iL+CDLC (0.1%BSA+2% chemical defined lipid component), 2iL+dep-
839 AX (deproteinized AX), and 2iLA. Scale bar, 25 μm. **b,** Western blotting assay to
840 evaluate expression levels of Eras, c-Myc, Dnmt3a and Dnmt31. **c,** Western blotting
841 assay to evaluate expression levels of Esrrb, Klf2, Kif 4 and Oct4. **d,** qRT-PCR
842 expression levels of the formative marker genes *Dnmt3b*, *Dnmt3l*, and *Lef1* in ESCs
843 cultured in 2iL, 2iL+CDLC, 2iL+dep-AX, or 2iLA. **e,** Karyotyping analyses of ESCs at
844 P12 after culture in 2iL, 2iL+BSA (0.1%fatty acid free BSA), 2iL+CDLC (0.1%BSA
845 +2%Chemical defined lipid component), 2iL+dep-AX (deproteinized AX), or 2iLA. **f,**
846 Schematic of the experiments using X^GX^T reporter ESCs to monitor the X chromosome
847 loss. **g,** FACS analyses of X chromosome loss for X^GX^T ESCs cultured in different

848 media. **h,** Flow cytometry analysis of the X^GX^T ESCs showing GFP+Tomato+ ESCs at
849 passage 15.

850 **Fig.4 | Lipid-induced formative pluripotency is maintained in concert with 2i. a,**
851 shown are representative colony morphologies of ESCs cultured in 2iL (CHIR+PD+LIF),
852 CL (CHIR+LIF), PL (PD+LIF), L (LIF) with or without 1%AlbuMAX (A) at passage 3 or 4.
853 Scale, 25 μm. **b,** the cell growth curves of ESCs cultured in 2iLA, CLA or PLA at
854 passage 3. ***P<0.001, t-test. **c,** FACS analysis of the mesendoderm differentiation
855 marker brachyury (T) positive cells at different time points after Activin A addition for
856 ESCs cultured in 2iL, 2iLA or L to test the responsiveness to directed differentiation. **d,**
857 Tetraploid complementation assay for two ESC lines cultured in 2iLA or LA. **e,**
858 Karyotyping analyses of ESCs cultured in different media with AlbuMax (+AX) or without
859 (-AX) after 15~16 passages. Normal karyotype/Total analysis metaphases. n=~20
860 metaphases for each condition. 2iL: CHIR+PD+LIF, CL: CHIR+LIF, PL: PD+LIF, L: LIF.
861 **f,** FACS analysis to evaluate the Zscan4 positive cell percentage using the Zscan4-
862 GFP and MERVL-tdTomato reporter ESC line cultured in different media at P1.

863 **Fig.5 | Mek/Erk signaling is essential for lipid induced formative transition. a-b,**
864 Western blotting for Erk1/2 and p-Erk1/2 proteins in ESCs cultured in 2iL or 2iLA at
865 passage 3 (a) or for Mek/Erk signaling related proteins in ESCs after switching 2iL to
866 2iLA (b). m, minutes; h: hours. **c,** qRT-PCR for the naive marker genes *Nanog*, *Prdm14*
867 and formative marker genes *Dnmt3b*, *Pim2* for *WT*, *Erk2*$^{-/-}$, *Erk2-Res* ESCs at passage
868 4 cultured in 2iL or 2iLA. *Erk2-Res*: *Erk2*-rescued in the *Erk1/2* mutant ESCs (Lentiviral-
869 based shRNA against *Erk1* in the *Erk2*$^{-/-}$ ESCs). n= 3 experiments.

870 ns, no significant difference, *P<0.05, **P<0.01, ***P<0.001, ****P<0.0001, student t-
871 test. **d-e,** Schematic illustration of the experimental design and ESC colony morphology
872 change (d), and qRT-PCR for the naive marker genes *Zfp42*, *Prdm14*, and the formative
873 marker genes *Dnmt3b*, *Pim2* for WT, and *Erk2* $^{-/-}$*Erk2-Res* (e) after 2i and LIF removal
874 for 72 hours. n= 3 experiments. **f-g,** FACS analysis of X^GX^T reporter female ESCs
875 cultured in SL2i, 2iL or 2iLA from P1 to over P15 (f) or in 2iL, 2iLA, 2iLA + VX-11e (Erk2
876 inhibitor) or CLA + VX-11e from P1 to P15 (g), CLA: CHIR 99021 +LIF+ AlbuMAX. **h,**
877 Karyotyping of the X^GX^T, *Erk2-/-*, *Mek1* $^{-/-}$*Mek2* $^{-/-}$ double knockout (*Mek1/2* dKO) PSCs
878 cultured in 2iLA over passage 15. n=~20 metaphases for each cell line.

879 **Fig.6 | Lipid-induced pluripotency transition is restrained through manipulating**
880 **Fgf/Erk signaling. a,** The colony morphology of ESCs cultured in 2iL at P3, 2iLA at
881 P15, reversing 2iLA at P12 to 2iL at P3 (R), 2iLA+iErk (1μM SCH772984, iErk) at P1
882 and 2iLA+iFgfr1-3(1μM AZD4547, iFgfr1-3) at P1. Scale, 25 μm. **b-c,** Heatmap for the
883 naive and formative genes based on bulk RNA-seq (b) or nucleotides analysis by LC-
884 MS. (c) for ESCs at P3 or P15 in 2iL, 2iLA or R-ESC (R, Reversing 2iLA at P12 to 2iL at
885 P3). n= 3 biological replicates. **d,** Western blotting for proteins for ESCs in 2iL or 2iLA at
886 P15 and R-ESCs at P3. **e,** FACS for the differentiation marker brachyury (T) positive
887 cells after adding Activin A after Day0, Day1, or Day2 embryoid body formation for
888 ESCs in 2iL or 2iLA at P6 and R-ESC (Reversing 2iLA at P3 to 2iL at P3). **f-i,** qRT-PCR
889 for the formative genes *Dnmt3b*, *Dnmt31*, *Lef1* (**f**), and the telomere maintenance gene
890 *Zscan4*. (**i**) or FACS for the differentiation marker T positive cells (**g**) or tetraploid
891 complementation (**h**) for ESCs cultured in 2iL,2iLA, iErk or iFgfr1-3. **P<0.01,
892 ***P<0.001, ***P<0.0001, student t-test. **(j)** Schematic summary of the pluripotency

893 transition or genomic stability between naive and formative states. 2i-ESCs maintain
894 naive state with genome instability, while supplement AlbuMAX (AX) in 2iL pushes
895 naive to formative state transition with genomic stability. This lipid induced pluripotency
896 transition is reversible by withdrawing AX from the 2iLA or by adding an additional p-Erk
897 specific inhibitor or Fgfr inhibitor in 2iLA.

898 **Fig.7 | Generation of male and female all-ESC mice from de novo derived ESCs**
899 **using AX-based medium. a,** Schematic illustration of the experimental design. **b,**
900 Tetraploid complementation assays for de novo derived ESCs (E3.5-E5.5 embryos) in
901 AX-based medium. F1(129B6): hybrid F1 crossed with C57B6 females to 129S1 male;
902 ICR: outbred strain; B6: inbred strain C57BL/6j; XX: female; XY: male. The numbers for
903 each bar represent the No. pups/ No. embryos transferred. **c,** Tetraploid
904 complementation assays for de novo derived ESCs (E3.5-E4.5 embryos) in CSA
905 medium. **d,** A litter of all-ESC mice from a male ESC line derived from E4.5 ICR
906 blastocysts in CSA medium. **e,** E5.5 blastocysts cultured in vitro (embryos hatching
907 from the zona pellucida). The ICM outgrowth on feeders in 2iLA (second panel). The
908 colonies of male fPSCs(third panel) or female fPSCs(fourth panel) derived from E5.5
909 blastocyst are shown in 2iLA at passage 3. Scale:100 μm.**f-g,** Karyotyping analyses of
910 the embryo-derived female ESCs at P20. **h,** Tetraploid complementation assays for
911 embryo-derived male and female ESCs. The numbers for each bar represent the No.
912 pups/ No. embryos transferred. **i,** A litter of pups from XY-4 male cell line is shown at
913 day 5 that was naturally delivered at term (9 pups/15 embryos transferred). **j,** A litter of
914 embryo-derived female fPSCs (XX-3) is shown at day 1 (6 pups/24 embryos
915 transferred). **k,** Adult female from the embryo-derived ESCs (XX-3). **l,** both male and

916 female mice generated from the embryo-derived ESCs are fertile and produce normal
917 litters. Bar scale in panel E: 100 μm.

918 **Extended data Fig.1 | AX promotes ESC proliferation and developmental potency.**

919 **a,** Representative colonies, cell growth curves and doubling times of ESCs cultured in
920 2il or 2iLA at P3, 15, and P20. Scale bar in panel a: 25 μm. **b,** Representative chimeras
921 derived from ESCs cultured in 2iL, 2iLA, or SL (serum+LIF) at P3. **c,** All-ESC pups from
922 ESCs (ESC-1) cultured in 2iLA at P14 and P21. **d,** Dot plots quantifying the all-ESC
923 pups obtained from ESCs (ESC-1) cultured in 2iL or 2iLA. **e,**one all-ESC pup obtained
924 from the ESCs (ESC-1) cultured in 2iLA for 43 passages, which is almost three months
925 in vitro.

926 **Extended data Fig.2 | AX maintains genomic stability of ESCs. a,** Karyotyping
927 analyses for the number of chromosomes of the ESCs cultured in 2il and 2iLA at P15.
928 **b,** Representative metaphase spread with trisomy 8 (41, XY, +8) from ESCs in 2iL at
929 P15. Arrow: Trisomy 8. **c,** Karyotyping analysis for trisomy 8 in 2iL or 2iLA at different
930 passages (n=~20 metaphases at each passage for 2iL or 2iLA). **d,** Karyotyping
931 analyses for the number of chromosomes of the ESCs cultured in 2il and 2iLA at P43. **e,**
932 Analysis for karyotype with chromosome loss in 2iL and 2iLA at different passages
933 (n=~20 metaphases at each passage for 2iL or 2iLA). **f,** the telomere length analyzed by
934 qPCR relative to a single copy gene(T/S) at passage 15 using three different ESC lines.
935 Statistics were with Student's t-test. **g,** Relative telomere length from P0 to P6,
936 ***P<0.001, ns, non-significant, based on t-test. **h,** Heatmap of Zscan4 related
937 transcripts from RNA-seq for ESCs cultured in 2iL or 2iLA at P3. **i,** FACS analysis to

938 evaluate the Zscan4 positive cell percentage using the Zscan4-GFP and MERVL-
939 tdTomato reporter cell line.

940 **Extended data Fig.3 | AX induces the transition of ESCs from naive to formative-**
941 **like pluripotency. a-b,** qRT-PCR for the naive or formative genes for ESCs cultured in
942 2iL, 2iLA, SL, or SL2i (a) or the formative genes in 2iL or 2iLA at P3 (b). **c,** Venn
943 diagram plot of differentially expressed genes (DEGs) between 2iL and 2iLA ESCs at p3
944 or p15. Overlapping DEGs with FDR<0.1 & abs (FC)>1 between P3 and P15 and GO
945 analysis for DEGs from bulk RNA-seq. n= three biological replicates for RNA-seq. **d,**
946 Gene expression heatmap of primed genes, the mESC (Naive), fPSC (Formative), and
947 EpiSC (Primed) are from published data [22].

948 **Extended data Fig.4 | Lipids in AlbuMAX impact intracellular metabolism.**

949 **a,** Schematic of the tricarboxylic acid (TCA) cycle and de novo lipogenesis. **b,** LC-MS
950 analysis of TCA cycle for ESCs cultured in SL, SL2i, 2iL or 2iLA. **c,** qRT-PCR for TCA
951 related enzyme genes in SL, SL2i, 2iL, 2iLA 24hr, 2iLA 48hr, or 2iLA P3. **d-e,** Western
952 blot (**d**) or qRT-PCR (**e**) for de novo lipogenesis related enzymes for ESCs in 2iL or
953 2iLA at P3. **f,** LC-MS analysis of the metabolites glycerol-3-phosphate or
954 phosphoethanolamine for ESCs in SL, SL2i, 2iL or 2iLA. **g,** LC-MS analysis of amino
955 acids for ESCs cultured in SL, SL2i, 2iL or 2iLA.

956 **Extended data Fig.5 | Formative-like pluripotency is maintained in concert with 2i.**
957 **a,** shown are representative colony morphologies of ESCs cultured in 2iLA
958 (CHIR+PD+LIF+AlbuMAX) or LA (LIF+AlbuMax). Scale, 25 μm. **b,** Formative

959 pluripotency marker genes *Dnmt3b*, *Lef1* and *Pou3f1* expression levels by qRT-PCR.
960 **P<0.01, ***P<0.001, ****P<0.0001, ns: non-significant, based on t-test. **c,** Karyotyping
961 analyses of trisomy 8 (41, XY, +8) for ESCs cultured in media with AlbuMAX (+AX) or
962 without (-AX) after 15~16 passages. Trisomy 8 karyotype/Total analysis metaphases.
963 n=~20 metaphases for each condition.

964 **Extended data Fig.6 | Fatty acid oxidation (FAO) is not required for lipid induced**
965 **pluripotency transition. a,** Schematic illustration of the experimental design for FAO
966 pathway inhibition. **b,** Colony morphology after FAO pathway inhibition. Etomoxir (ETO,
967 100μM), Trimetazidine (TMZ, 200μM). **c,** Formative gene Dnmt3b expression after FAO
968 pathway inhibition. Etomoxir (ETO, 100μM), Trimetazidine (TMZ, 200μM). **d,** Carnitine
969 Palmitoyltransferase 1A (Cpt1a) deletion in mESCs, homologous deletion (the deletion
970 region 125 bp spanning between exon3 and intron 3). **e,** Colony morphology after Cpt1a
971 deletion. **f,** Formative gene *Dnmt3b* expression (qRT-PCR) after Cpt1a deletion.

972 **Extended data Fig.7 | Mek/Erk signaling is essential for lipid-induced pluripotency**
973 **transition. a,** qRT-PCR for *Dnmts* transcript levels in ESCs after switching 2iL to 2iLA
974 at different time points. **b,** Western blotting for Erk1/2 in *WT*, *Erk2*$^{-/-}$, *Erk1/2* mutant,
975 *Erk2-Res1* or *Erk2-Res2* ESCs in 2iL or 2iLA. Erk2-Res: Erk2-rescued in the *Erk1/2*
976 mutant ESCs (Lentiviral-based shRNA against Erk1 in the *Erk2*$^{-/-}$ ESCs). **c-d,** qRT-PCR
977 for the *Erk1/2* target gene *Spry4* (c), and the formative marker genes *Wnt8a* and *Lef1*
978 for *WT*, *Erk2*$^{-/-}$, *Erk1/2* mutant and *Erk2-Res* ESCs after 4 passages cultured in 2iL or
979 2iLA(d). **e-f,** Schematic illustration of the *Mek1/2* dKO ESCs generation and the
980 experimental design (e), and Western blotting for validating the deletion Mek1/2 protein

981 of the *Mek1/2* dKO ESCs cultured in 2iL or 2iLA (f). **g,** qRT-PCR for the naive genes
982 *Nanog*, *Prdm14* and formative genes *Dnmt3b*, *Pim2* for *WT*, *Mek1*$^{f/f}$*Mek2*$^{-/-}$, *Mek1/2* dKO
983 ESCs after 5 passages in 2iL or 2iLA. *P<0.05, **P<0.01, ***P<0.001, ****P<0.0001, t-
984 test. **h,** Western blotting for the p-Mek1/2 or p-Erk1/2 protein level in *Mek1*$^{-/-}$*Mek2*$^{-/-}$ dKO
985 and its control PSCs. **i-j,** Colony morphology change (i) and qRT-PCR for naive gene
986 *Nanog* and formative gene *Dnmt3l* (j) after swtiching 2iL to 2iLA at different time points
987 for *WT*, M*ek1*$^{f/f}$*Mek2*$^{-/-}$, *Mek1/2* dKO, *Erk2*$^{-/-}$ or *Erk2-Res* ESCs.

988 **Extended data Fig.8 | Fgf/Erk signaling manipulation in AX-based media and ESC**
989 **derivation. a,** heatmap showing transcript levels of the MAPK/ERK pathway related
990 genes based on bulk RNA-seq for ESCs cultured in 2iL or 2iLA at P3. n=3 biological
991 replicates. **b,** qRT-PCR or Western blotting assays (P3) of Fgf5 for ESC cultured in 2iL
992 or 2iLA. **P<0.01, student t-test. **c,** the growth curve for the proliferation rates for ESCs
993 cultured in 2iL, 2iLA, 2iLA+iErk, or 2iLA+iFgfr media. **d,** shown are nine pups derived
994 from ESCs cultured in 2iLA+iFgfr1-3 from one surrogate recipient mouse (9 pups/ 20
995 embryos transferred) by tetraploid complementation. **e,** karyotyping analyses of ESCs
996 cultured in 2iLA, 2iLA+iErk, or 2iLA+iFgfr media at P12. **f,** the ICM outgrowth from a F1
997 (129B6) or ICR E3.5 embryo on feeders at day 6 cultured in 2iLA or CSA. g, all-ESC
998 pups generated for the CSA derived ESCs from F1 or B6 E3.5 blastocysts, and for CSA
999 cultured ICR ESCs.

1000 **Extended data Fig 9. Schematic illustrating the dual role of lipids on genome**
1001 **stability and pluripotency of mouse embryonic stem cells.** Lipids directly stimulate
1002 Mek-mediated Erk2 phosphorylation which leads to exit of naïve state and

1003 establishment of formative pluripotency for ESCs cultured in 2iLA medium. Lipid
1004 metabolism reduces the lipogenesis and amino acid biosynthesis and promotes non-
1005 canonical TCA metabolites associated with the exit of naïve pluripotency. However, lipid
1006 metabolism through β-oxidation is dispensable for transition from naïve to formative
1007 state. Lipids enhance the expression of ZSCAN4, DNMT3s and Prps2 that are involved
1008 in maintenance of telomere length, DNA methylation, and nucleotide pool, therefore
1009 promoting genome stability. Stimulation of Erk2 activity by lipids also alleviates X
1010 chromosome loss and trisomy 8 for ESCs cultured in 2iLA medium. The dual role of
1011 lipids on genome stability and pluripotency facilitates the preservation of full
1012 developmental potency of murine ESCs for both sexes during long-term culture in vitro.

1013

1014

1015 **Methods**

1016 **Mice and embryos.** Animals were housed and cared for according to a protocol approved
1017 by the IACUC of Weill Cornell Medical College (Protocol number: 2014-0061). Wild-type
1018 ICR mice were purchased from Taconic Farms (Germantown, NY); the 129S1 and C57B6
1019 mice were purchased from Jackson Laboratories. Females were super-ovulated at 6–8
1020 weeks with 0.1 ml CARD HyperOva (Cosmo Bio Co., Cat. No. KYD-010-EX) and 5 IU
1021 hCG (Human chorionic gonadotrophin, Sigma-Aldrich) at intervals of 48 hours. The
1022 females were mated individually to males and checked for the presence of a vaginal plug
1023 the following morning. Plugged females were sacrificed at 1.5 days post hCG injection to
1024 collect 2-cell embryos. Embryos were flushed from the oviducts with advanced KSOM
1025 (Cat # MR-101-D, Millipore) and cultured in KSOM medium in an incubator under 5%
1026 CO2 at 37°C until blastocyst stage for ESC injection.

1027 **Blastocyst injection and tetraploid complementation.** ESCs were trypsinized,
1028 resuspended in ESC medium and kept on ice. A flat tip microinjection pipette was used
1029 for ESC injections. ESCs were collected at the end of the injection pipette and 10–15
1030 cells were injected into each blastocyst. The injected blastocysts were kept in KSOM
1031 until embryo transfer. Typically, ten injected blastocysts were transferred into each
1032 uterine horn of 2.5 dpc pseudo-pregnant ICR females. Tetraploid embryos were
1033 generated using 2-cell stage embryos flushed from the oviducts. The 2-cell embryos
1034 were subjected to electrofusion to induce tetraploidy. Fused embryos were moved to
1035 new KSOM micro drops covered with mineral oil and cultured to blastocyst stage until
1036 ESC injection.

1037 **2iL medium and 2iLA medium.** 2iL medium contains 1:1 mixture of DMEM/F12 and
1038 Neurobasal media supplemented with N2 (Gibco™, 17502048) and B27 (Gibco™,
1039 17504044), L-glutamine (Millipore, TMS-002-C), 2-mercaptoethanol (Millipore, ES-007-
1040 E), 1x penicillin/streptomycin (Millipore, TMS-AB-2C) and LIF (Sigma-Aldrich,
1041 ESG1107), 1 μM PD0325901 (Sigma or Stemolecule) and 3 μM CHIR99021 (Sigma).
1042 2iLA medium was made from 2iL medium supplemented with 1% AlbuMax (W/V,
1043 Gibco™, 11020039).

1044 **ESC derivation and culture.** ESCs were derived from hybrid F1 fertilized embryos
1045 derived by crossing C57BL/6J females and 129S1 males. The ESC derivation medium
1046 contains KnockOut™ Dulbecco's modified Eagle's medium (Gibco, 10829-018), 20%
1047 KnockOut™ Serum Replacement (Gibco, 10828), 10^3 IU recombinant mouse LIF
1048 (Millipore, ESG1107), 2mM L-glutamine (Millipore, TMS-002-C), 1x
1049 penicillin/streptomycin (Millipore, TMS-AB-2C), 1x non-essential amino acids (Millipore,
1050 TMS-001-C), 1x nucleosides for ES cells (Millipore, ES-008-D), 1x β-mercaptoethanol
1051 (Millipore, ES-007-E), 1μM PD98059 (Promega, V1191) and 3 μM CHIR99021 (Sigma).
1052 The medium used for ESCs derivation was 2iLA medium which is standard 2iL medium
1053 supplemented with 1% AlbuMAX (w/v). Briefly, E3.5-E5.5 blastocysts were collected
1054 from the plugged females treated with CARDova/hCG. The zona pellucida was removed
1055 by briefly exposing the blastocysts to Tyrode's acidic solution (Millipore, MR-004).
1056 Blastocysts with dissolved zona pellucida were picked up with a mouth pipette and
1057 washed in KSOM medium for 2-3 times. Blastocysts were then placed individually on
1058 96-well plate on feeder layers with the derivation medium. After 5-7 days' culture, the
1059 ICM outgrowth originated from the blastocysts were trypsinized in 20 μL 0.025% trypsin

1060 solution (Millipore, SM-2004-C) for 5 min, and 200 μL culture medium was added to
1061 stop the reaction. Colony expansion of ESCs proceeded from 48-well plates to 6-well
1062 plates with feeder cells. Cell aliquots were cryopreserved using Cell Culture Freezing
1063 Medium (Millipore, ES-002-D) and stored in liquid nitrogen. ESCs were routinely
1064 expanded and maintained as following: Before passaging, the plates were treated with
1065 EmbryoMax™ 0.1% gelatin solution (Cat # ES-006-B, Millipore) for at least 10 min, and
1066 the ESC culture media were added to the wells after removal of gelatin solution. ESCs
1067 were then placed on the wells with proper cell density and usually cultured for 2 days
1068 before next passaging.

1069 **Mutant ESC lines.** The $X^{GFP}X^{Tomato}$ ESC line was a gift from Dr. Konrad Hochedlinger
1070 and the *Erk1/2* mutant ESC lines were obtained from Dr. Danny Reinberg with the
1071 permission from Dr. Sylvain Meloche. The Nanog-GFP cell line was a gift from Dr.
1072 Rudolf Jaenisch. The dual reporter ESC line (MERVL-tdTomato and ZSCAN4c-GFP)
1073 was a gift from Dr.Jianlong Wang. The *Mek1*$^{f/f}$ *Mek2*$^{-/-}$ iPSC cell line was a gift from Dr.
1074 Konrad Hochedlinger, the *Mek1*$^{-/-}$*Mek2*$^{-/-}$ iPSC cell line was generated by adding Cre
1075 Recombinase Adenovirus (Vectorbiolabs, Cat. No: 1710) into *Mek1*$^{f/f}$ *Mek2*$^{-/-}$ iPSCs.
1076 After transfection, the cells were sorted for GFP expression by flow cytometry and the
1077 sorted cells were expanded; single cells were picked and expanded for identifying the
1078 *Mek1/2* double knockout cell line. The *Cpt1a*$^{-/-}$ ESC cell line was generated by CRISPR-
1079 Cas9 using Neon transfection system, the sgRNA sequencing is
1080 CACCACGATAAGCCAGCTGGAGG.

1081 **Deproteinization of AlbuMAX.** AlbuMAX deproteinization was performed as described
1082 in Garcia-Gonzalo and Izpisu´ a Belmonte [4]. Briefly, 0.5 mL of a 100X solution of

1083 Trypsin from bovine pancreas (Sigma) was added to 50 mL of a 10% w/v solution of
1084 AlbuMAX in base medium (AX-Trypsin solution) without supplement and incubated for
1085 30 minutes at 37℃ in a water bath. Then, 0.5ml of a 100X solution of Soybean Trypsin
1086 inhibitor was added to the AX-Trypsin solution and incubated at room temperature for
1087 30 minutes. The deproteinized AlbuMAX solution was sterile filtered and added to 2iL to
1088 a final concentration of 1% w/v. Fatty acid-free BSA (Sigma, A3803) was added to 2iL
1089 medium to a final concentration of 0.1% w/v. Chemically defined lipid concentrate
1090 (CDLC, Thermo Fisher Scientific, 11905031) was added at a concentration 2% v/v into
1091 2iL media.

1092 **Karyotype analysis.** Briefly, cultures were treated with Colcemid at final concentration
1093 of 0.05 µg/m. Following 60-90 min incubation, cells were trypsinized according to
1094 standard procedures, washed twice in 1X PBS, incubated in 0.075M KCl for 10 minutes
1095 at 37°C and fixed in chilled methanol-acetic acid (3:1). The fixed cell suspension was
1096 then dropped onto slides, stained in 0.08 µg/ml DAPI in 2xSSC for 3 minutes and
1097 mounted in antifade solution (Vectashield, Vector Labs). The stained slides were
1098 scanned using a Nikon E800 epifluorescence microscope equipped with imaging and
1099 digital karyotyping system from Applied Spectral Imaging (Carlsbad, CA). For each
1100 sample a minimum of 20 metaphases were captured. All metaphases were fully
1101 karyotyped and analyzed for chromosomal instability. The experiments were performed
1102 at the MSKCC Molecular Cytogenetics Core Facility.

1103 **RNA-sequencing.** Total genomic DNA or RNA was prepared from cultured ESCs using
1104 the DNeasy Blood and tissue kit (QIAGEN) or RNeasy Mini Kit (QIAGEN), respectively,
1105 following the manufacturer's instructions. The RNA concentration and integrity were

1106 measured using a NanoDrop 2000 (Thermo Fisher Scientific) and Agilent 2100
1107 Bioanalyzer (Agilent), respectively. The integrity of RNA was indicated by the RNA
1108 integrity number (RIN). RNA samples with sufficient concentration and RIN greater than
1109 8.0 were further prepared for cDNA library preparation using poly-A selection and
1110 unstranded library preparation using a Truseq library preparation kit (Illumina) according
1111 to manufacturer's instructions. DNA library was then sequenced using a NovaSeq 6000
1112 - S1 Flow Cell, with pair-end reads, 2x50 cycles at the Weill Cornell Genomics Core
1113 Facility. Reads from RNA-seq were aligned to mouse genome version mm10 using
1114 TopHat. Gene counts were obtained using featureCounts to sort bam files, and only
1115 unique-mapping reads were used. Genes without any expression counts in any sample
1116 were discarded. Differentially gene expression analysis was performed using DESeq2
1117 (version 1.4.5) R package that normalizes gene count data to transcription per million
1118 (TPM), and then detects differentially expressed genes (DEG) between 2i-ESCs and
1119 AX-ESCs groups (FDR < 0.1).

1120 **RRBS-sequencing.** Reduced Representation Bisulfite Sequencing is a modification of
1121 the original RRBS protocol [64] and the in-house developed ERRBS method [65] for
1122 base-pair resolution methylation sequencing analysis based on the use of a restriction
1123 enzyme to enrich for CpG fragments. 150 ng of RNA-free genomic DNA per sample
1124 was used for RBBS sequencing at Weill Cornell Medicine Epigenomics Core.
1125 Concentration of double stranded DNA (dsDNA) was determined using Qubit
1126 Fluorometer, Perkin Elmer Labchip GX or agarose gel electrophoresis to determine
1127 molecular weight. 100 million (M) read per sample on a single end read flow cell with
1128 100 sequencing cycles (SR100) was used for differential methylation analysis. FASTQ

1129 files were generated by bcl2fastq (V2.17) and filtered for pass filter reads based on
1130 Illumina's chastity filter. Sequencing adapters were trimmed by FLEXBAR (V2.4) [66],
1131 genomic alignments using Bismark (V0.14.4) [67] and Bowtie2 (V2.2.5) [68] to reference
1132 mm10, and per base CpG methylation metrics were calculated with a custom PERL
1133 script. CpGs at a minimum threshold coverage of 5 reads were used for downstream
1134 analysis.

1135 **Western blotting assays.** Cells were lysed into 1× SDS loading buffer (50 mM Tris-HCl
1136 pH 6.8,5% β-mercaptoethanol, 2% SDS, 0.01% bromophenol blue, 10% glycerol)
1137 followed by sonication (Bioruptor, 2 × 30 s at high setting). Proteins were resolved on a
1138 5–15% gradient Tris–glycine SDS–PAGE gel and semi-dry-transferred to nitrocellulose
1139 membranes. The following primary antibodies were used at the indicated dilutions:
1140 Zscan4 (Millipore, AB4340); Dnmt3a (Abcam, ab2850), Dnmt3b (Abcam, ab2851),
1141 GAPDH (CST, 5174, 1:10,000); Erk1/2 (CST, 4695); p-Erk1/2 (CST, 9101); Nanog
1142 (CST, D2A3 XP®). Horseradish peroxidase (HRP)-conjugated secondary antibodies
1143 and the ECL prime western blotting system (GE Healthcare, RPN2232) were used for
1144 detection of primary antibodies. For the Erk1/2 &p-Erk1/2 or Mek1/2&p-Mek1/2, the
1145 equivalent samples were loaded on two parallel gels synchronously and then the gels
1146 were transferred to nitrocellulose membranes synchronously. Chemiluminescent signals
1147 were captured with a digital camera (Kindle Biosciences).

1148 **Quantitative real-time PCR.** ESCs were homogenized in RNA lysis buffer (RLT buffer,
1149 Qiagen) with 1% β-mercaptoethanol. RNA was then prepared following the RNeasy
1150 protocol (QIAGEN). DNA was digested using DNase I (QIAGEN) during the RNA
1151 extraction processes. The RNA concentration was measured by NanoDrop (Thermo

1152 Fisher Scientific). RNA (200 ng) was used for cDNA conversion using qScript Super Mix
1153 (Quanta Biosciences). After cDNA dilution with double-distilled H_2O at a 1:10 ratio, the
1154 qPCR reaction was prepared by mixing the gene-specific primers and PowerUp SYBR
1155 Green Master Mix (Thermo Fisher Scientific;cat. no. A25778). qPCR was run using a
1156 QuantStudio 3 machine (Thermo Fisher Scientific).

1157 **Flow cytometry.** The attached cells were washed with 1x PBS and dissociated with
1158 Trypsin-EDTA (0.025%) at room temperature for 5 min. The same volume of Defined
1159 Trypsin Inhibitor (Gibco, R007100) was added to the detached cell suspension,
1160 incubated at room temperature for 5 min, and then washed with 1xPBS and centrifuged
1161 for the cell pellet. Samples without fluorescent reporter were used as the negative
1162 control. Finally, the cell pellet was suspended in MACS (1x PBS with 2mM EDTA and
1163 0.5% BSA) with DAPI and applied to a flow cytometer for analysis (FACSymphony™ A5
1164 or Fortessa , BD) at the Weill Cornell Medicine Flow Cytometry Core Facility .

1165 **Telomere length measurement.** The ScienCell Absolute Mouse Telomere Length
1166 Quantification qPCR Assay Kit (AMTLQ, Catalog #M8918) was used to directly
1167 measure the average telomere lengths. The telomere primer set recognizes and
1168 amplifies telomere sequences. The single copy reference (SCR) primer set recognizes
1169 and amplifies a 100 bp-long region on mouse chromosome 10 and serves as reference
1170 for data normalization. A genomic DNA sample with known telomere length served as a
1171 reference for calculating the telomere length of target samples.

1172 **ESC directed differentiation.** For mesendoderm differentiation, embryoid bodies (EBs)
1173 were formed in serum free differentiation media (SFD). SFD consisted of 75% IMDM

1174 (Gibco), 25% Ham's F12 (Corning cellgro), 0.5X N2 (Gibco), 0.5X B27 (Gibco), 0.05%
1175 BSA (Gibco), 0.5mM Ascorbic Acid (Sigma), 2mM Glutamine (Corning), 0.45 mM
1176 monothioglycerol (Sigma), 100U/mL Penicillin and 0.1 mg/ml Streptomycin (Corning).
1177 On the first day of differentiation, cells were dissociated with Accutase (Sigma) and
1178 plated at 40,000 cells/ml in Petri dishes. Activin A (R&D Systems or Peprotech) was
1179 added at designed timepoints: day0 (0h), day1(24h), and day2 (48h) at a final
1180 concentration of 75 ng/ml. For Brachyury staining, EBs were dissociated with Accutase,
1181 fixed with 2% paraformaldehyde (Electron Microscopy Sciences) and stained with anti-
1182 Brachyury PE-conjugated Antibody (R&D) for 2h according to manufacturer instructions.
1183 After two washes, cells were analyzed using an Attune Nxt flow cytometer (Life
1184 Sciences).

1185 **Liquid chromatography–mass spectrometry (LC-MS)**. For all metabolite analyses,
1186 cells were seeded in 2iL or 2iLA media in 6-well plates. Metabolites were extracted with
1187 1 ml ice-cold 80% methanol supplemented with 20 mM deuterated 2-hydroxyglutarate
1188 (D-2-hydroxyglutaric- 2,3,3,4,4-d5 acid (d5-2HG)) as an internal standard. After
1189 overnight incubation at -80℃, lysates were harvested and centrifuged at 21,000g for 20
1190 min to remove protein. Extracts were dried in an evaporator (GenevacEZ-2Elite) and
1191 resuspended by incubation at 30℃ for 2h in 50 ml of 40 mg ml^{-1} methoxyamine
1192 hydrochloride in pyridine. Metabolites were further derivatized by addition of 80 ml of
1193 MSTFA plus 1% TMCS (Thermo Scientific) and 70 ml ethyl acetate (Sigma) and
1194 incubated at 37℃ for 30 min. Samples were analyzed using an Agilent 7890A GC
1195 coupled to Agilent 5975C mass selective detector in the Metabolomics & Lipidomics
1196 facility at The Rockefeller University. The GC was operated in split less mode with

1197 constant helium gas flow at 1 ml/min. One microliter of derivatized metabolites was
1198 injected onto an HP-5MS column and the GC oven temperature ramped from 60℃ to
1199 290℃ over 25 min. Peaks representing compounds of interest were extracted and
1200 integrated using MassHunter software (Agilent Technologies) and then normalized to
1201 both the internal standard (d5-2HG) peak area and the protein content of duplicate
1202 samples as determined by a BCA protein assay (Thermo Scientific).

1203

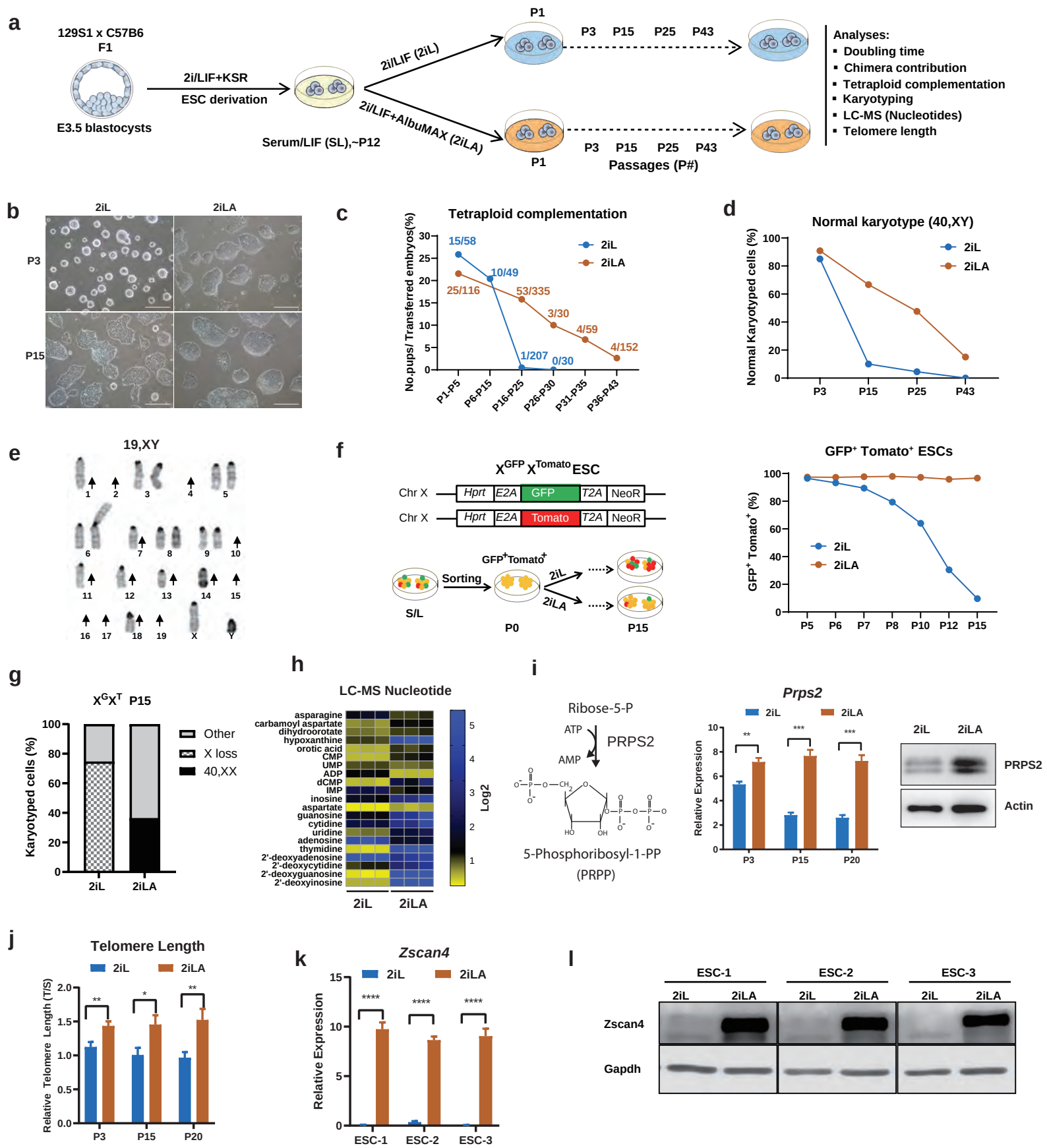

Fig.1|AX improves developmental potential and genomic stability of mouse ESCs. a, Schematic illustration of the experimental design. **b,** Colony morphology for ESCs cultured in 2iL or 2iLA at passage 3 or passage 15. Scale, 25 µm. **c,** Developmental potential assessed by tetraploid complementation. The numbers at each timepoint represent total No. pups/No.embryos transferred. **d-e,** Analysis for normal karyotype (**d**) in 2iL and 2iLA at different passages (n=~20 metaphases at each passage for 2iL or 2iLA).Representative severe chromosome loss (**e**) in 2iL at P43. Arrow: Chromosome loss. **f,** FACS analysis of X^GX^T reporter female ESC cultured in 2iL or 2iLA. The double reporter positive cells indicate both X chromosomes are maintained. **g,** Karyotyping of the X^GX^T ESCs cultured in 2iL and 2iLA at passage 15. **h,** LC-MS analysis of nucleotide pools for ESCs cultured in 2iL and 2iLA (P3). **i,** Prps2 expression levels by qRT-PCR assay or Western blot assay. **P<0.01,***P<0.001, t-test. **j,**The telomere length analyzed by qRT-PCR relative to a single copy gene(T/S) for the ESC cultured in 2iL or 2iLA at different passages.*P<0.05, **P<0.01,t-test. **k-l,** Relative *Zscan4* transcript (**k**) or protein (**l**)levels by qRT-PCR analysis or Western blot assay.****P<0.0001, t-test.

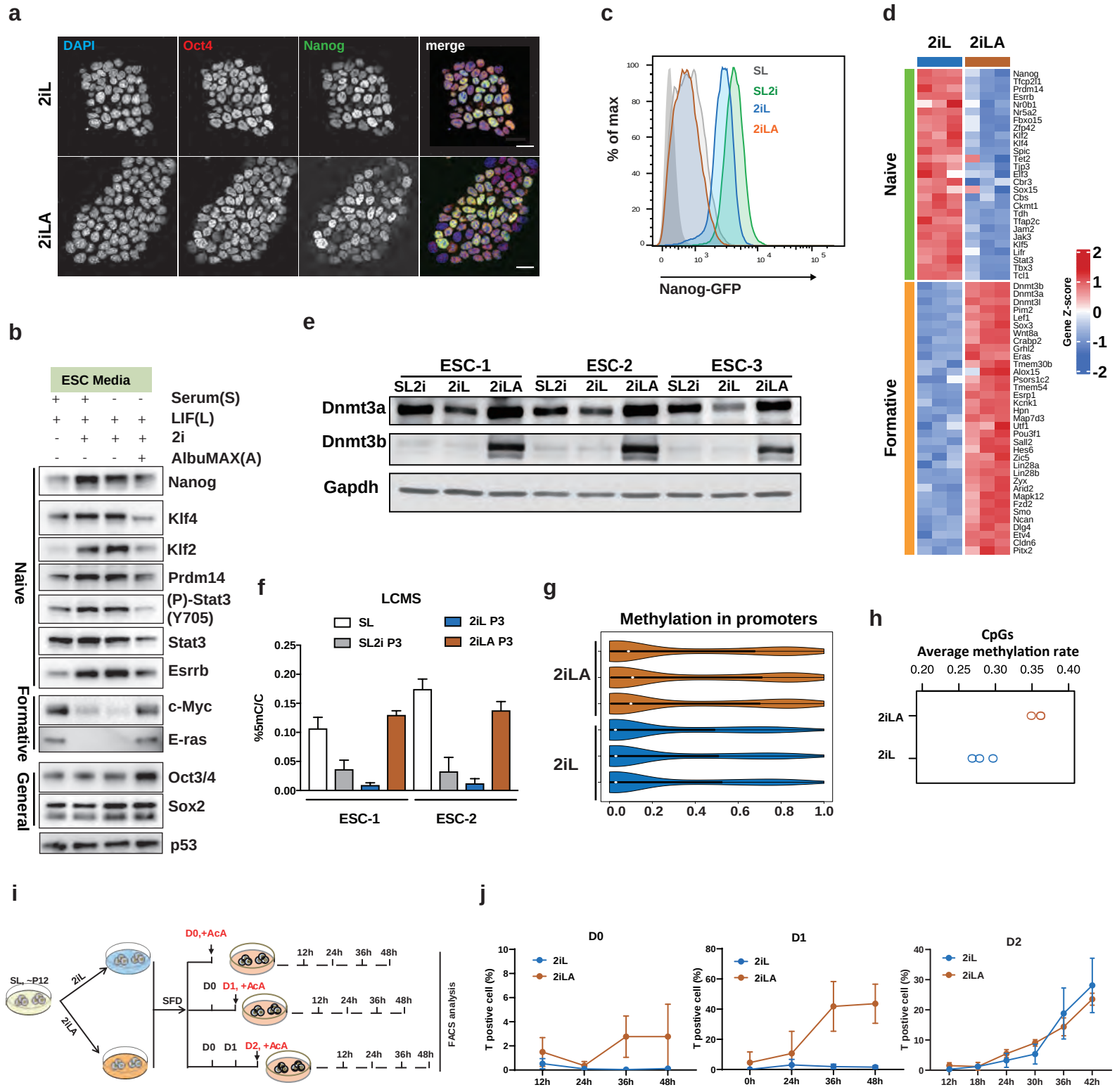

Fig.2 | AX induces the transition of ESCs from naive to formative-like pluripotency. a, Immunostaining for Oct4(red) and Nanog(green) of ESCs cultured in 2il or 2iLA. DAPI (Blue) for cell nuclei. **b,** Western blotting of the naive,formative or general pluripotency marker protein level in SL,SL2i,2iL and 2iLA. **c,** FACS analysis using a GFP:Nanog ESC reporter line, the GFP fluorescence intensity is decreased in 2iLA. **d,** Heatmap of transcript levels from bulk RNA-seq for the naive and formative genes cultured in 2iL or 2iLA at P3. Three different ESC lines for biological replicates. **e,** Dnmt3a/b levels demonstrated by western blotting assays. **f,** LC-MS showing the global levels of 5mC/C ration in genomic DNA from ESCs cultured in different media. **g,** Violin plots of the DNA methylation distribution rate at promoter regions in ESCs cultured in 2iL or 2iLA at P3 from Reduced representation bisulfite sequencing (RRBS). Three biological replicates. **h,** RRBS for quantification of the average global methylation rate in all CpGs . Three biological replicates. **i,** Schematic of the assay to test responsiveness to Activin A for differentiation. **j,** FACS analysis of the mesendoderm differentiaiton marker brachyury(T) positive cells at different time pionts after Activin A(AcA) addition at Day0(D0),Day1(D1) or Day2(D2) embryoid body formation. D0, D2 Two biological replicates, D1 Three biological replicates.

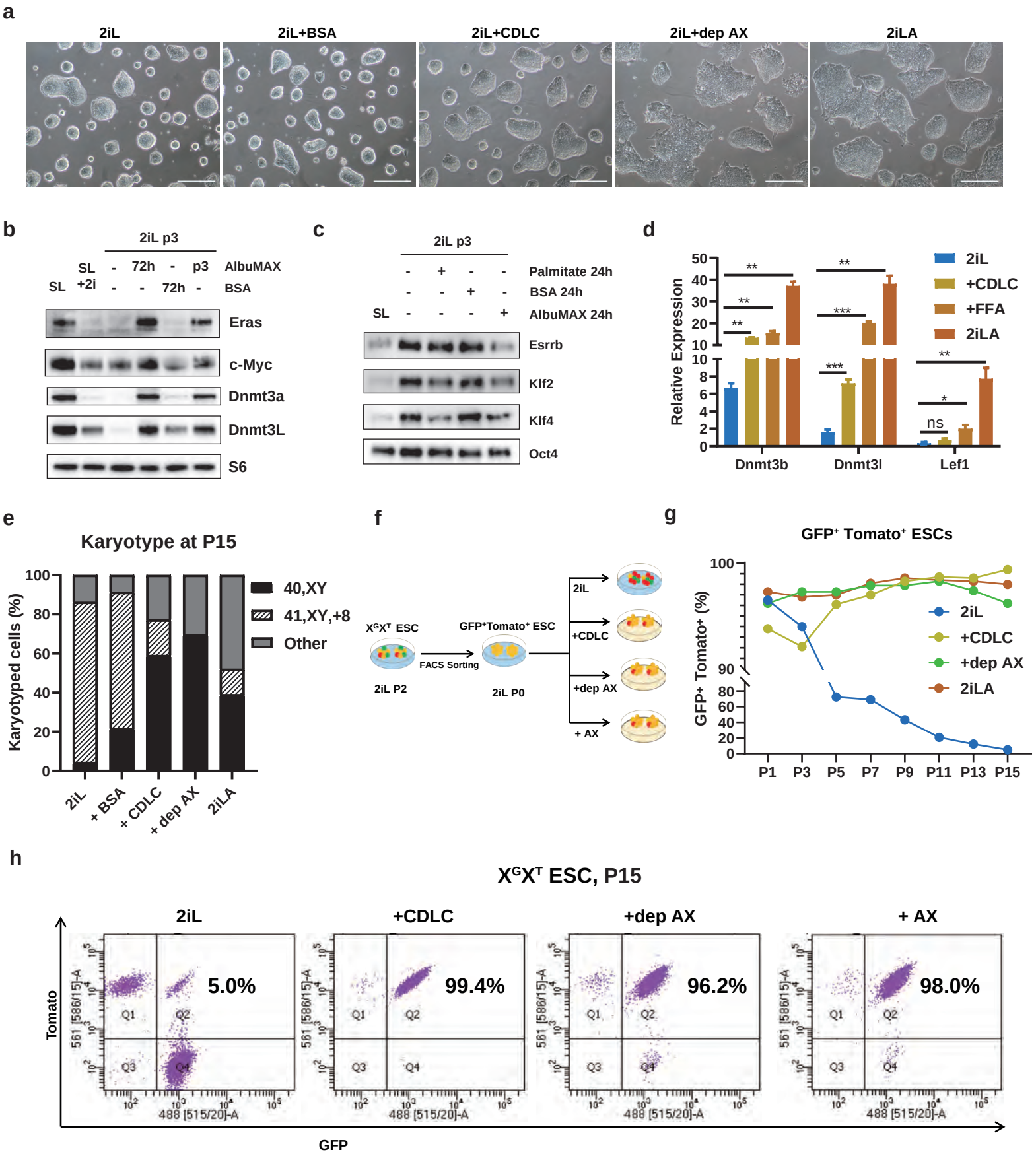

Fig.3 | Lipids in AX drive the pluripotency transition and promote genomic stability. a, The colony morphology is shown for ESCs cultured in 2iL, 2iL+BSA (0.1%fatty acid free BSA), 2iL＋CDLC(0.1%BSA+ 2%Chemical defined lipid component),2iL+dep-AX (deproteinized AX), and 2iLA. Scale bar, 25 μm. **b,** Western blotting assay to evaluate expression levels of Eras, c-Myc, Dnmt3a and Dnmt31. **c,** Western blotting assay to evaluate expression levels of Esrrb, Klf2, Kif 4 and Oct4. **d,** qRT-PCR expression level of the formative marker genes *Dnmt3b, Dnmt3l,* and *Lef1* in ESC cultured in 2iL, 2iL＋CDLC, 2iL+dep-AX, and 2iLA. **e,** Karyotyping analyses of ESCs at P12 after culture in 2iL, 2iL+BSA (0.1%fatty acid free BSA), 2iL＋CDLC(0.1%BSA + 2%Chemical defined lipid component), 2iL+dep-AX(deproteinized AX), and 2iLA. **f,** Schematic of the experiments using X^GX^T reporter ESCs to monitor the X chromosome loss. **g,** FACS analyses of X chromosome loss for X^GX^T ESCs cultured in different media. **h,** Flow cytometry analysis of the X^GX^T ESCs showing $GFP^+Tomato^+$ ESCs at passage 15.

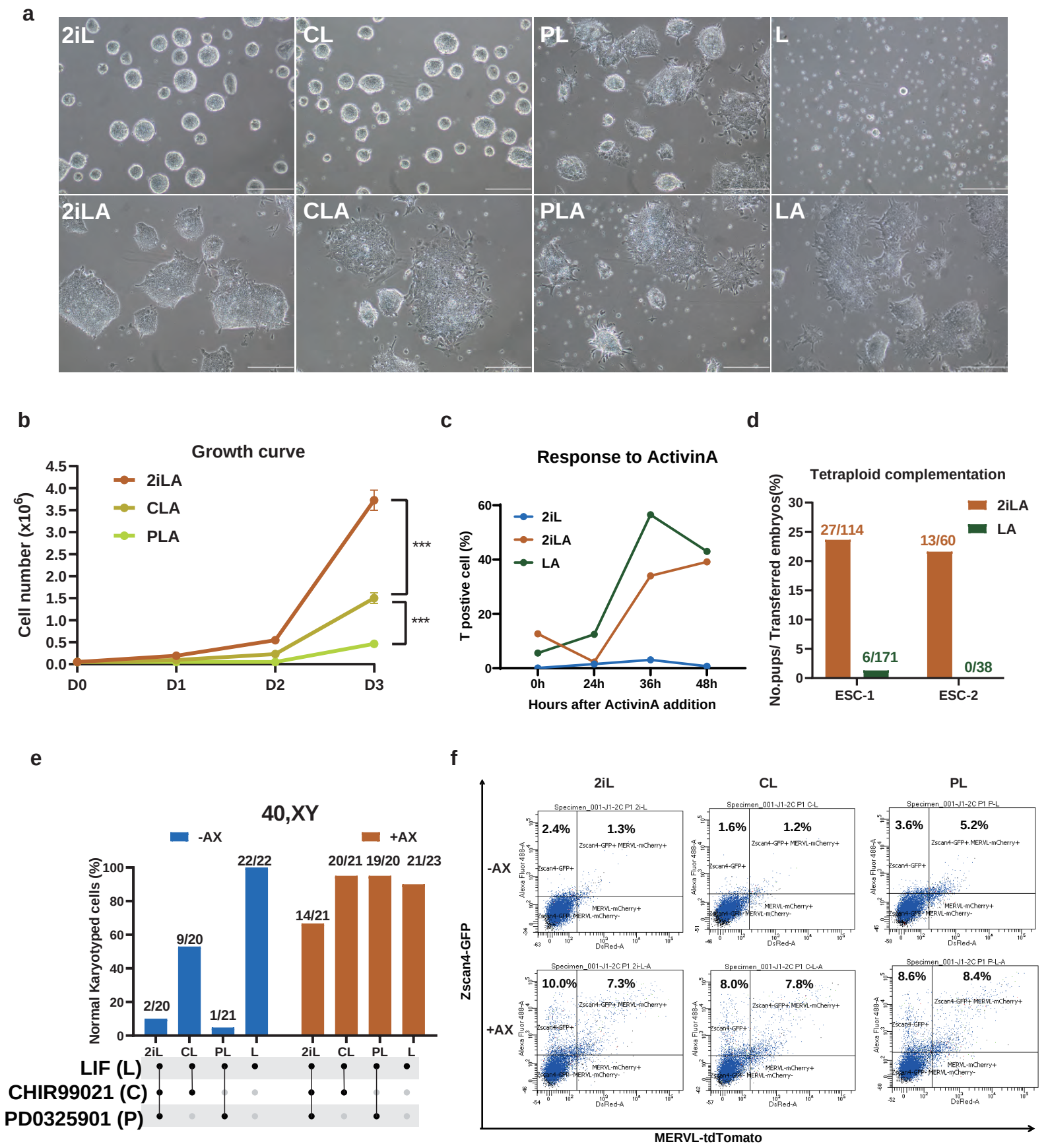

Fig.4 | Lipids maintain full pluripotency in concert with 2i but genomic stability independently. a, Shown are representative colony morphologies of ESCs cultured in 2iL(CHIR+PD+LIF), CL(CHIR+LIF), PL(PD+LIF), L(LIF) without or with 1%AlbuMAX (A) at passage 3 or 4. Scale, 25 µm. **b,** The cell growth curve of ESCs cultured in 2iLA,CLA and PLA at passage 3. ***P<0.001, t-test. **c,** FACS analysis of the mesendoderm differentiaiton marker brachyury(T) positive cells at different time pionts after Activin A addition for ESCs cultured in 2iL, 2iLA or L to test the responsiveness to direct differentiation. **d,**Tetraploid complementation assay for two ESC lines cultured in 2iLA or LA. **e,** Karyotyping analyses of ESCs cultured in different media with AlbuMax (+AX) or without it (-AX) after 15~16 passages. Normal karyotype/Total analysis metapahseses. n=~20 metaphases for each condition. 2iL: CHIR+PD+LIF, CL: CHIR+LIF, PL: PD+LIF, L:LIF. **f,** FACS analsysis to evaluate the Zscan4 postitive cell percentage using the Zscan4-GFP and MERVL-tdTomato reporter ESC line cultured in different media at P1.

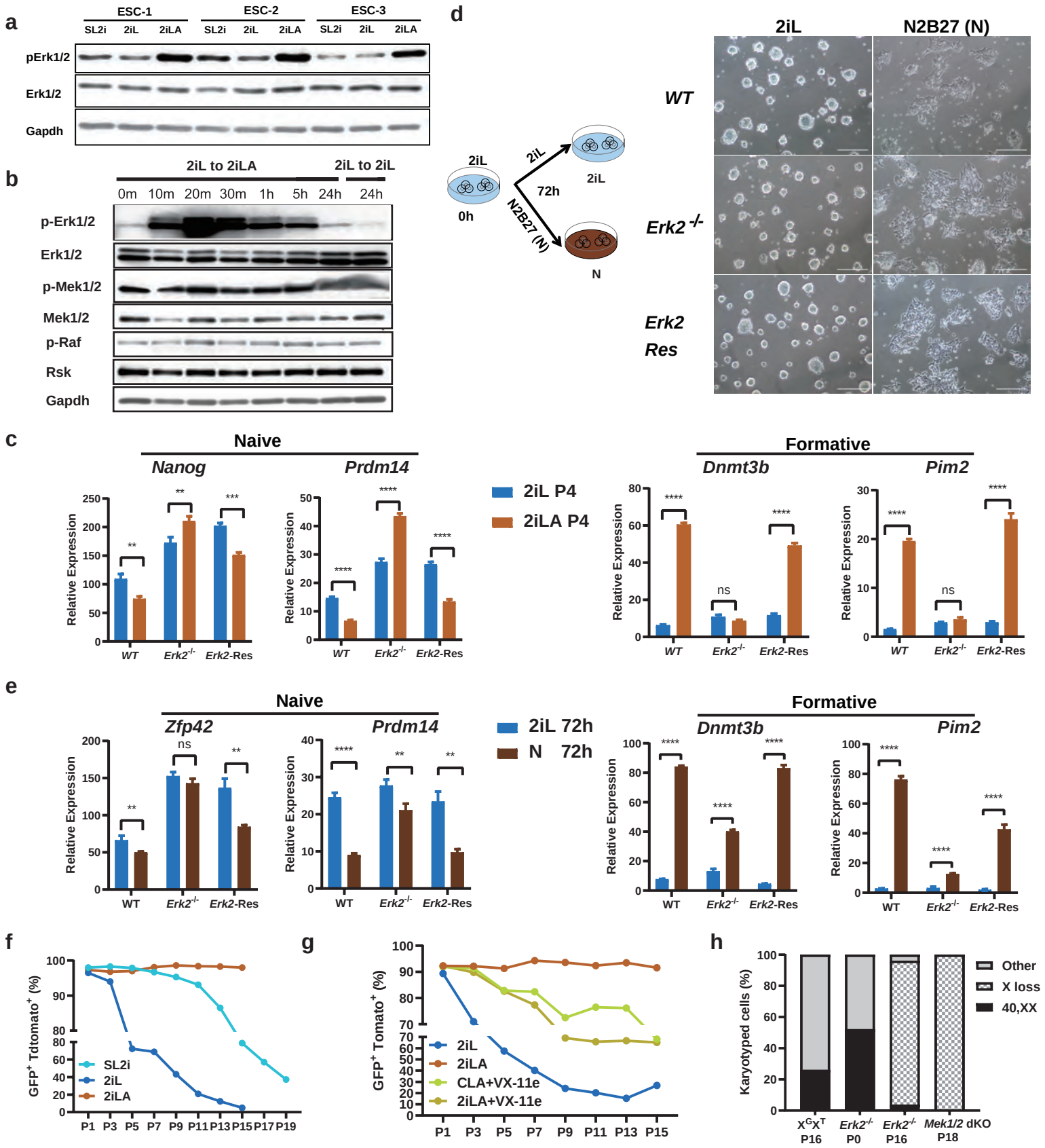

Fig.5 | Mek/Erk signaling is essential for lipid induced formative transition and maintained female ESC chromosome X stability. a-b, Western blotting for Erk1/2 and p-Erk1/2 proteins in ESCs cultured in 2iL or 2iLA at passage3 (**a**) or for Mek/Erk signaling related proteins in ESCs after switching 2iL to 2iLA(**b**). m, mintunes; h:hours. **c,** qRT-PCR for the naive marker genes *Nanog, Prdm14* and formative marker genes *Dnmt3b*,*Pim2* for *WT*, *Erk2* $^{-/-}$, *Erk2*-Res ESCs at passage4 cultured in 2iL or 2iLA. *Erk2*-Res: *Erk2*-rescued in the *Erk1/2* mutant ESCs (Lentiviral-based shRNA against *Erk1* in the *Erk2* $^{-/-}$ ESCs).Triplicate of the experiments. ns, no significant difference, *P<0.05,**P<0.01, ***P<0.001, ****P<0.0001, student t-test. **d-e,** Schematic illustration of the experimental design and ESC colony morphology change(**d**), and qRT-PCR for the naive marker genes *Zfp42, Prdm14,* and the formative marker genes *Dnmt3b*,*Pim2* for *WT*, and *Erk2* $^{-/-}$, *Erk2*-Res (**e**) after 2i and LIF removal for 72 hours. Triplicate of the experiments. **f-g,** FACS analysis of X^GX^T reporter female ESC cultured in SL2i, 2iL or 2iLA from P1 to over P15(**f**) or in 2iL, 2iLA, 2iLA + VX-11e (Erk2 inhibitor) or CLA + VX-11e from P1 to P15 (**g**),CLA: CHIR 99021 +LIF+AlbuMAX. **h,** Karyotyping of the X^GX^T, *Erk2*$^{-/-}$, *Mek1*$^{-/-}$*Mek2*$^{-/-}$ double knockout (*Mek1/2* dKO) PSCs cultured in 2iLA over passage 15. n=~20 metaphases for each cell line.

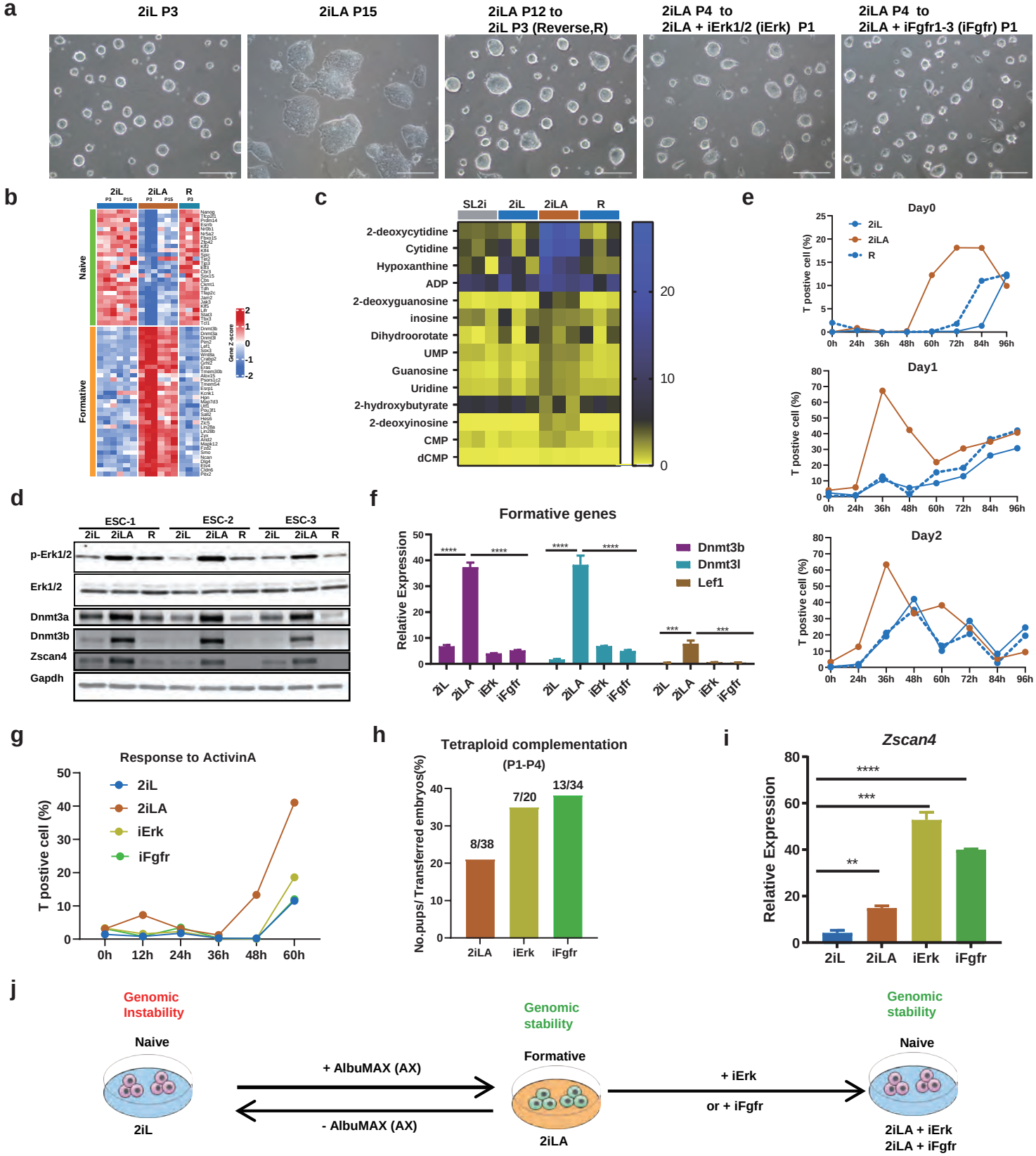

Fig.6 | Lipid-induced formative pluripotency is reversible by manipulating Fgf/Erk signaling. a, The colony morphology of ESCs cultured in 2iL at P3, 2iLA at P15, reversing 2iLA at P12 to 2iL at P3 (R), 2iLA+iErk1/2(1μM SCH772984,iErk) at P1 and 2iLA+iFgfr1-3(1μM AZD4547, iFgfr) at P1. Scale, 25 μm **b-c,** Heatmap for the naive and formative genes based on bulk RNA-seq (**b**) or nucleotides analysis by LC-MS (**c**) for ESCs at P3 or P15 in 2iL, 2iLA and R-ESC (R,Reversing 2iLA at P12 to 2iL at P3). 3 biological replicates **d,** Western blotting for proteins for ESCs in 2iL or 2iLA at P15 and R-ESCs at P3. **e,** FACS for the differentaition marker brachyury(T) positive cells after adding Activin A after Day0,Day1,or Day2 embryoid body formation for ESCs in 2iL or 2iLA at P6 and R-ESC(Reversing 2iLA at P3 to 2iL at P3). **f-i,** qRT-PCR for the formative genes *Dnmt3b*, *Dnmt31*, *Lef1*(**f**), and the telomere maintenance gene *Zscan4*(**i**) or FACS for the differentaition marker T positive cells (**g**) or tetraploid complementation(**h**) for ESCs cultured in 2iL,2iLA, iErk and iFgfr. **P<0.01, ***P<0.001,***P<0.0001,student t-test **j,** Schematic summary of the pluripotency transition or genomic stability between naive and formative states. 2i-ESCs maintain naive state with genome unstability, while supplement AlbuMAX (AX) in 2iL pushes naive to formative state transition with genomic stability. This lipid induced pluripotency transition is reversible by withdrawing AX from the 2iLA or by adding an additional p-Erk specific inhibitor or Fgfr inhibitor in 2iLA.

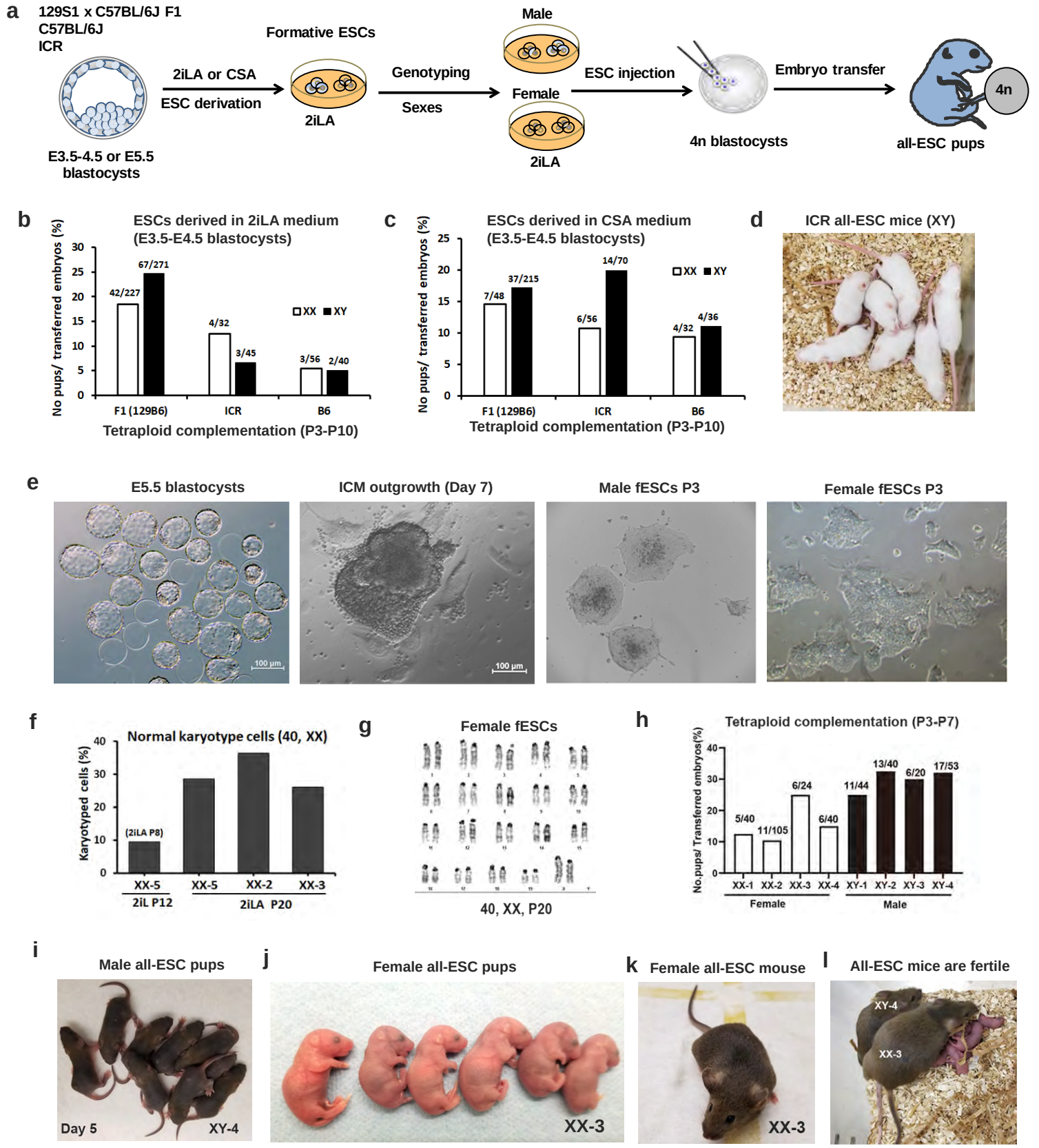

Fig.7 | Generation of all-ESC mice from both sex de novo derived ESCs by AX-based medium. **a,** Schematic illustration of the experimental design. CSA:CHIR+SCH772984+LIF+AlbuMAX **b-c,** Tetraploid complementation assays for de novo derived ESCs (E3.5-E4.5 blastocysts) in 2iLA (**b**)or CSA (**c**)medium. F1(129B6): hybrid F1 crossed with C57B6 females to 129S1 male; ICR: outbred strain; B6: inbred strain C57BL/6j; XX: female; XY: male. The numbers for each bar represent the No. pups/ No. embryos transferred. **d,** A litter of all-ESC mice from a male ESC line derived from E4.5 ICR blastocysts in CSA. **e,** E5.5 blastocysts cultured in vitro (embryos hatching from the zona pellucida). The ICM outgrowth on feeders in 2iLA (second panel). The colonies of male fESCs(third panel) or female fESCs(fourth panel) derived from E5.5 blastocyst are shown in 2iLA at passage 3. Scale:100 μm. **f-g,** Karyotyping analyses(**f**) and representative image (**g**) of the embryo-derived female fESCs at P20. **h,** Tetraploid complementation for embryo-derived male and female fESCs. The numbers for each bar represent the No. pups/ No. embryos transferred. **i,** A litter of day 5 pups from male fESCs (XY-4) was naturally delivered (9 pups/15 embryos transferred). **j,** A litter of day 1 pups from female fESCs (XX-3) (6 pups/24 embryos transferred). **k,** Adult female from the fESCs (XX-3). **l,** Both male and female mice generated from the fESCs are fertile and produce normal litters.

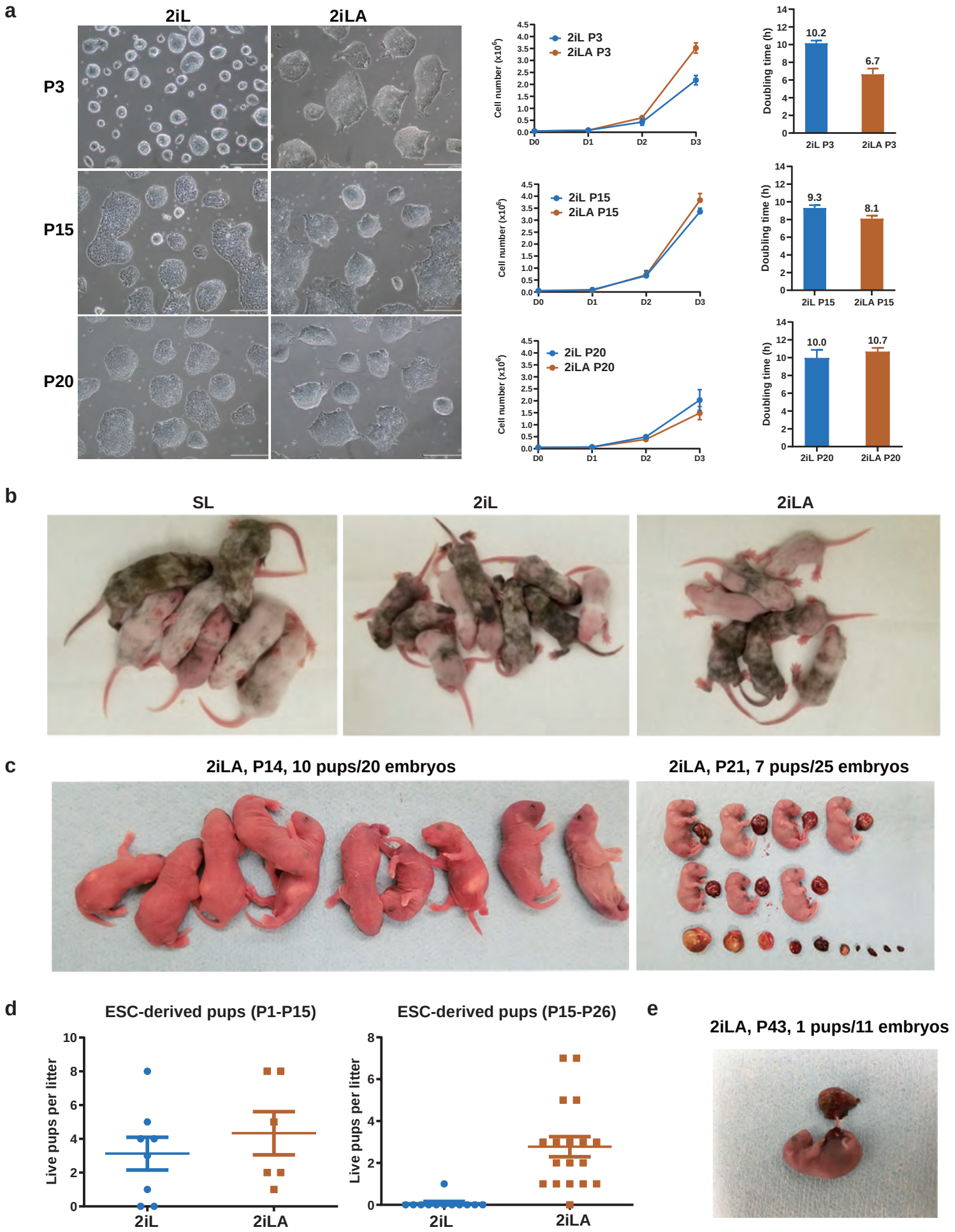

Extended Data Fig.1 | AX promotes ESC proliferation and prolongs the deveolopmetal potency. **a,** Representative colonies, the cell growth curve and doubling times of ESCs cultured in 2il and 2iLA at P3, P15, and P20. Scale bar in panel a: 25 μm. **b,** Representative chimeras derived from ESCs cultured in 2iL, 2iLA, or SL (serum+LIF) at P3. **c,** All-ESC pups from ESCs (ESC-1) cultured in 2iLA at P14 and P21. **d,** Dot plots quantifying the all-ESC pups obtained from ESCs (ESC-1) cultured in 2iL or 2iLA .**e,** One all-ESC pup obtained from the ESCs (ESC-1) cultured in 2iLA for 43 passages, which is almost three months in vitro.

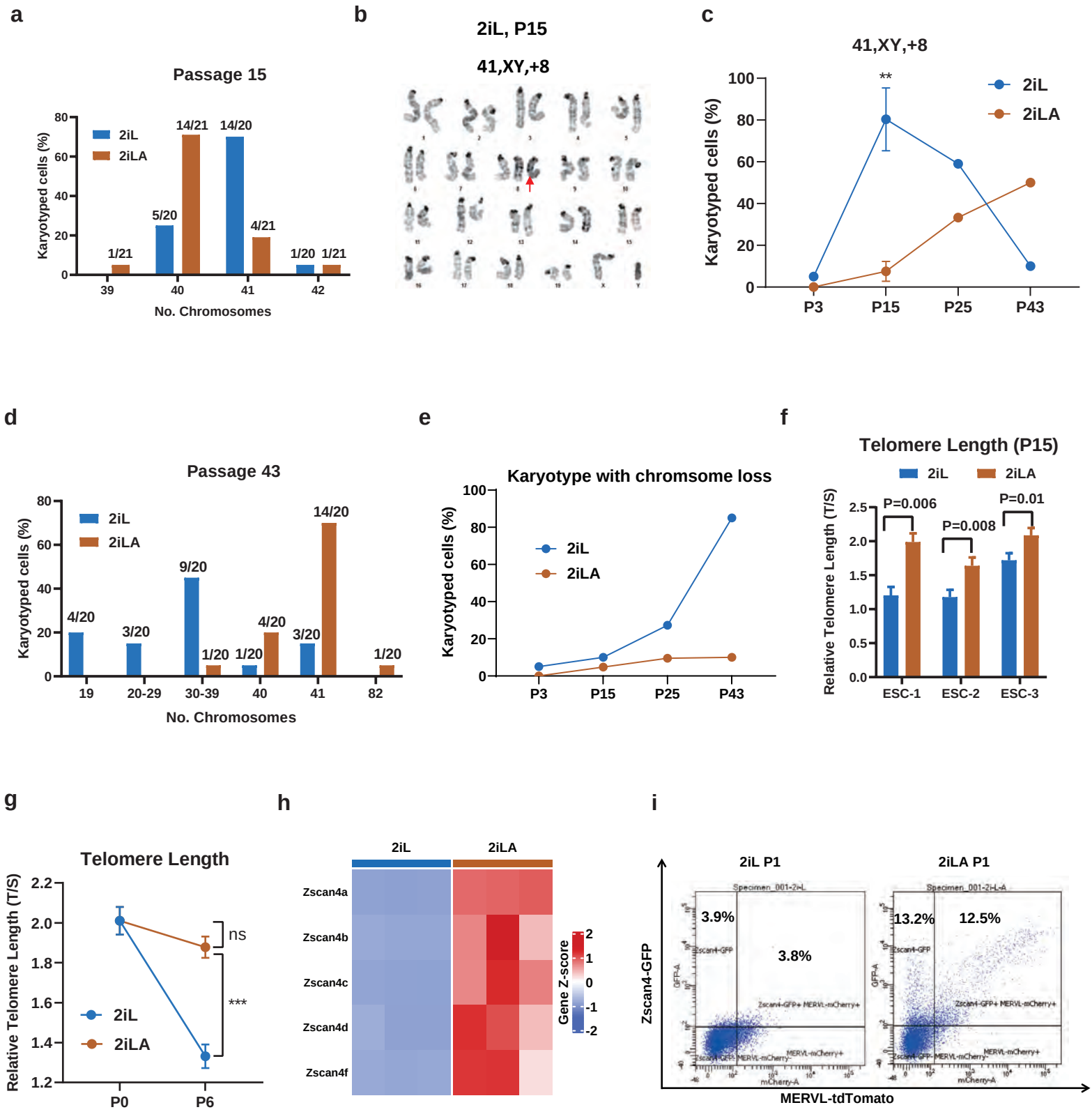

Extended data Fig.2 | AX postphones the trisomy 8 occurrence and maintains longer telomere. **a,** Karyotyping analyses for the number of chromosomes of the ESCs cultured in 2il and 2iLA at P15. **b,** Representative metaphase spread with trisomy 8 (41,XY,+8) from a ESC in 2iL at P15. Arrow:Trisomy 8 **c,**Karyotyping analysis for trisomy 8 in 2iL or 2iLA at different passages (n=~20 metaphases at each passage for 2iL or 2iLA). **d,** Karyotyping analyses for the number of chromosomes of the ESCs cultured in 2il and 2iLA at P43. **e,** Analysis for karyotype with chromosome loss in 2iL and 2iLA at different passages (n=~20 metaphases at each passage for 2iL or 2iLA). **f,**The telomere length analyzed by qPCR relative to a single copy gene(T/S) at passage 15 using three different ESC lines. Student t-test. **g,** Relative telomere length from P0 to P6,***P<0.001, ns, non significance, t-test. **h,** Heatmap of *Zscan4* related transcripts from RNA-seq for ESCs cultured in 2iL or 2iLA at P3. **i,** FACS analsysis to evaluate the Zscan4 postitive cell percentage using the Zscan4-GFP and MERVL-tdTomato reporter cell line.

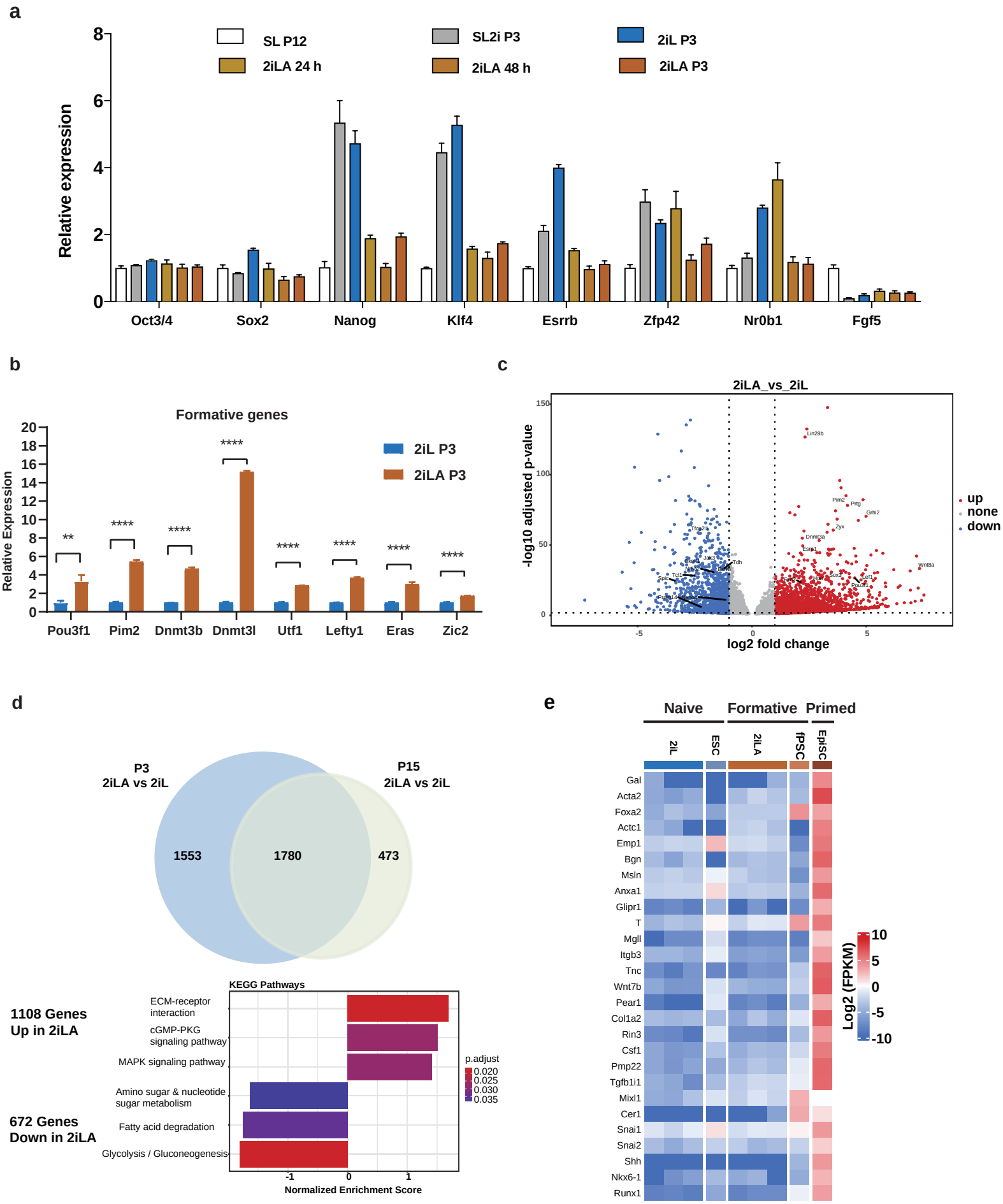

Extended data Fig.3 | AX induces the transition of ESCs from naive to formative-like pluripotency. **a-b,** RT-qPCR for the naive or formative genes for ESCs cultured in 2iL, 2iLA, SL, or SL2i (**a**) or the formative genes in 2iL or 2iLA at P3 (**b**). **c,** Volcano plot showing expression fold changes for differentially expressed genes (DEGs) between 2iL and 2iLA at P3. Blue, upregulated in 2iL; Red, upregulated in 2iLA **d,** Venn diagram plot of differentially expressed genes (DEGs) between 2iL and 2iLA ESCs at p3 or p15. Overlapping DEGs with padj<0.01 & abs(log_2FC)>1 between P3 and P15 and GO analysis for DEGs from bulk RNA-seq. Three biological replicates for RNA-seq. **e,** Gene expression heatmap of primed genes, the mESC(Naive), fPSC(Formative), and EpiSC(Primed) are from published data [Wang et al., 2021b].

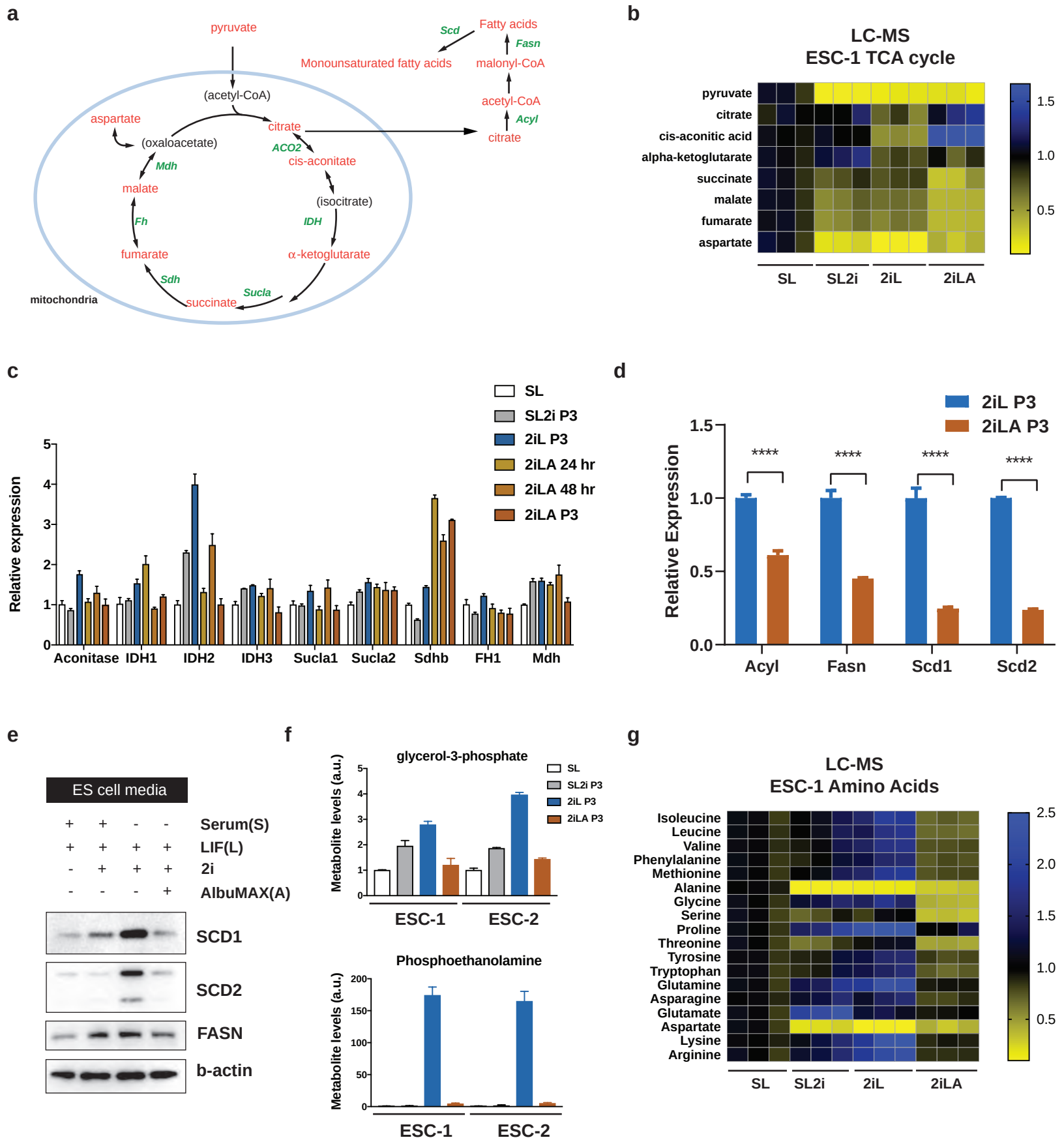

Extended Data Fig.4 | Lipids in AlbuMAX impact intracellular metabolism. a, Schematic of the tricarboxylic acid (TCA) cycle and de novo lipogenesis. **b,** LC-MS analysis of TCA cycle for ESCs cultured in SL, SL2i, 2iL and 2iLA. **c,** qRT-PCR for TCA related enzyme genes in SL, SL2i, 2iL, 2iLA 24hr, 2iLA 48hr, 2iLA P3. **d-e,** Western blot(**d**) or qRT-PCR(**e**) for for de novo lipogenesis related enzymes for ESCs in 2iL or 2iLA at P3. **f,** LC-MS analysis of the metabolites glycerol-3-phosphate or phosphoethanolamine for ESCs in SL,SL2i,2iL and 2iLA. **g,** LC-MS analysis of amino acids for ESCs cultured in SL, SL2i, 2iL and 2iLA.

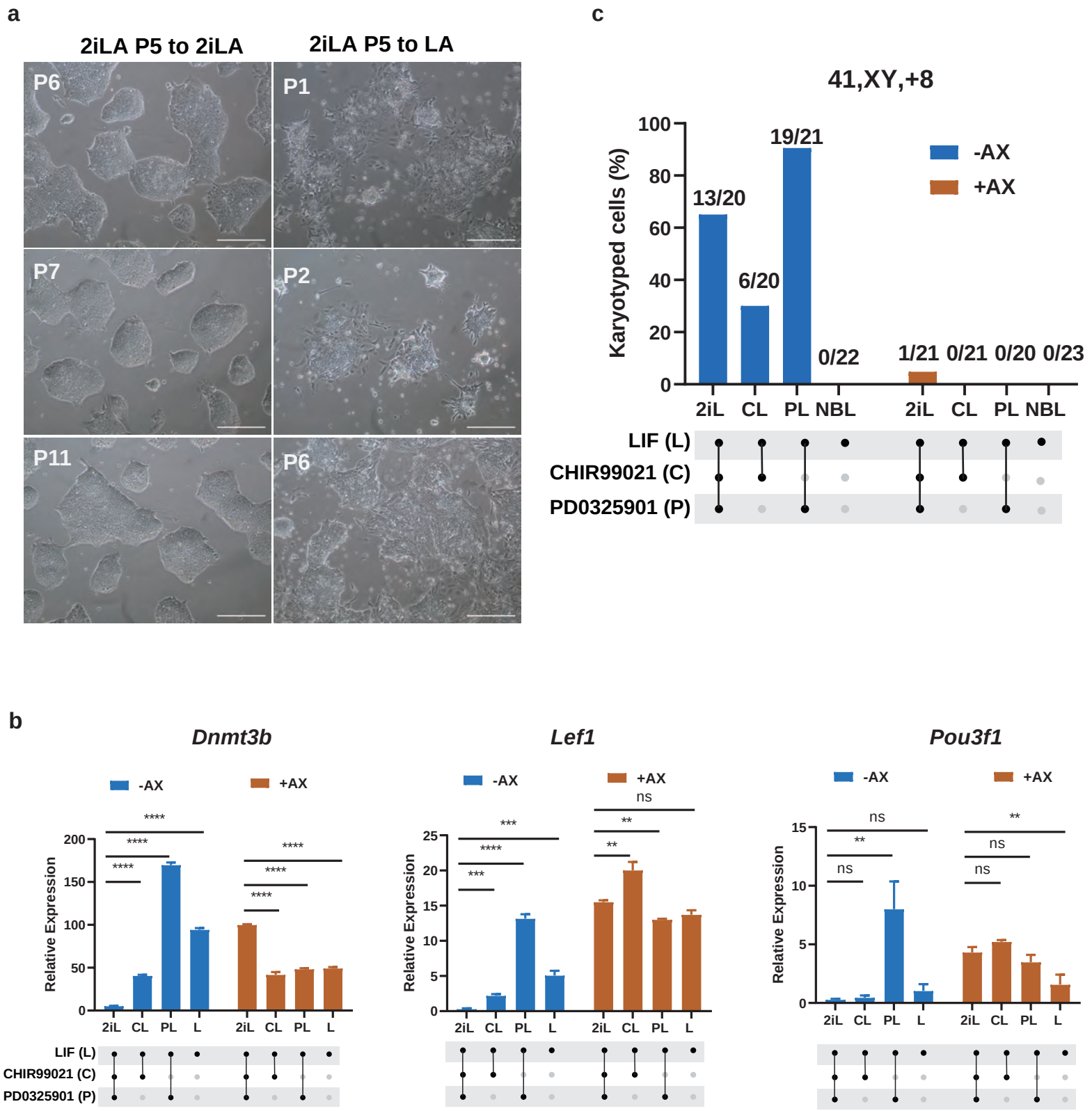

Extended Data Fig.5 | Lipids in concert with 2i are responsible for formative pluripotency maintenance, but independent of 2i for trisomy 8 prevention. a, Shown are representative colony morphologies of ESCs cultured in 2iLA (CHIR+PD+LIF+AlbuMAX) or LA(LIF+AlbuMax). Scale, 25 µm. **b,** Formative pluripotency marker genes *Dnmt3b*, *Lef1* and *Pou3f1* expression levels by qRT-PCR. **P<0.01,***P<0.001,****P<0.0001, ns: non significance, t-test. **c,** Karyotyping analyses of trisomy 8 (41,XY,+8) for ESCs cultured in media with AlbuMAX (+AX) or without it (-AX) after 15~16 passages. Trisomy8 karyotype/Total analysis metapahseses. n=~20 metaphases for each condition.

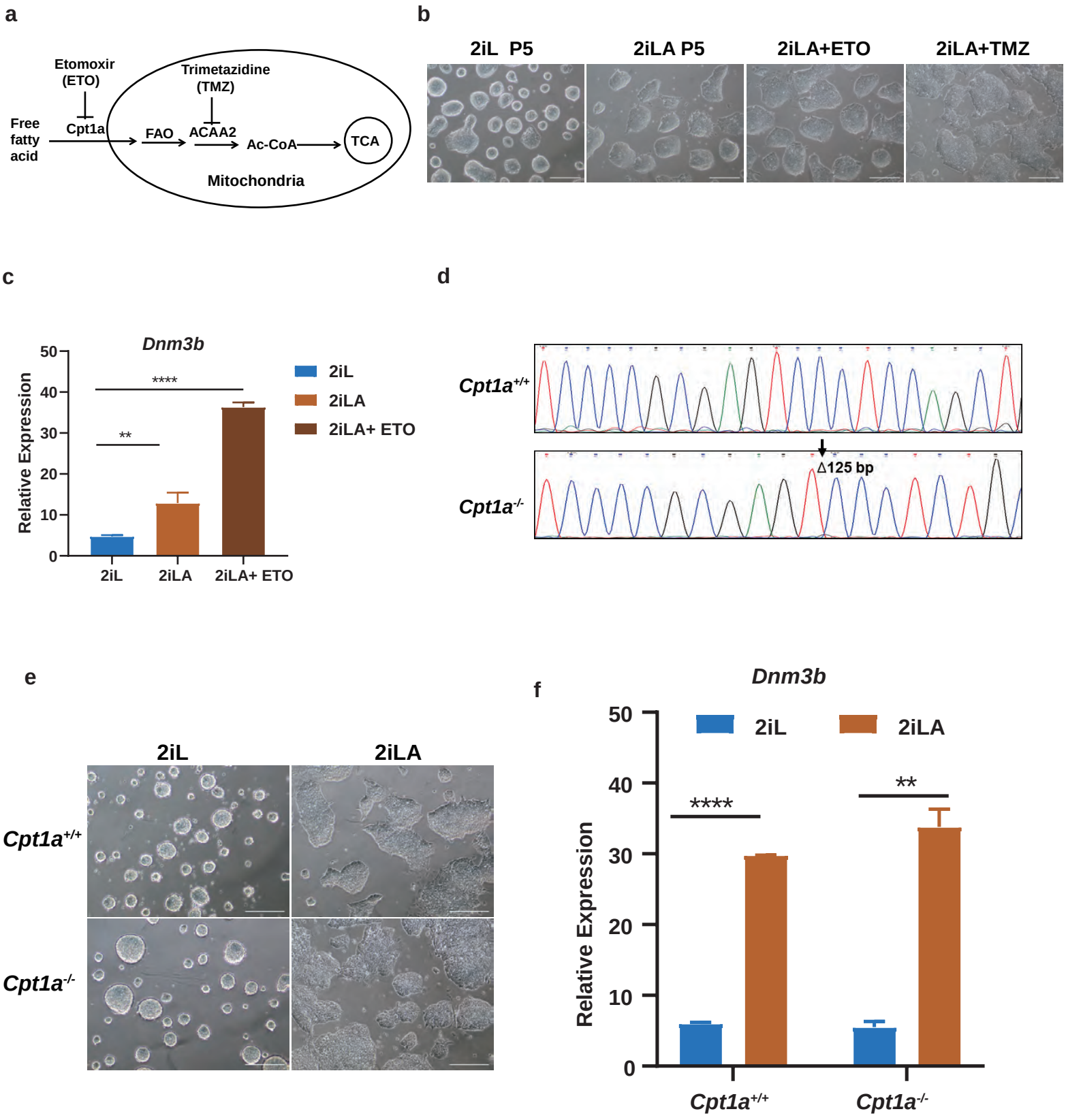

Extended data Fig.6 | Fatty acid oxidation (FAO) pathway is not invovled in lipid induced formative transition. a,Schematic illustration of the experimental design for FAO pathway inhibition. **b,** Colony morphology after FAO pathway inhibition. Etomoxir (ETO, 100μM), Trimetazidine (TMZ, 200μM). **c,**Formative gene *Dnmt3b* expression after FAO pathway inhibition. Etomoxir (ETO, 100μM), Trimetazidine (TMZ, 200μM). **d,** Carnitine Palmitoyltransferase 1A (*Cpt1a*) deletion in mESCs, homologous deletion (the deletion region 125bp spanning between exon3 and intron 3). **e,** Colony morphology after *Cpt1a* deletion. **f,**Formative gene *Dnmt3b* expression after *Cpt1a* deletion.

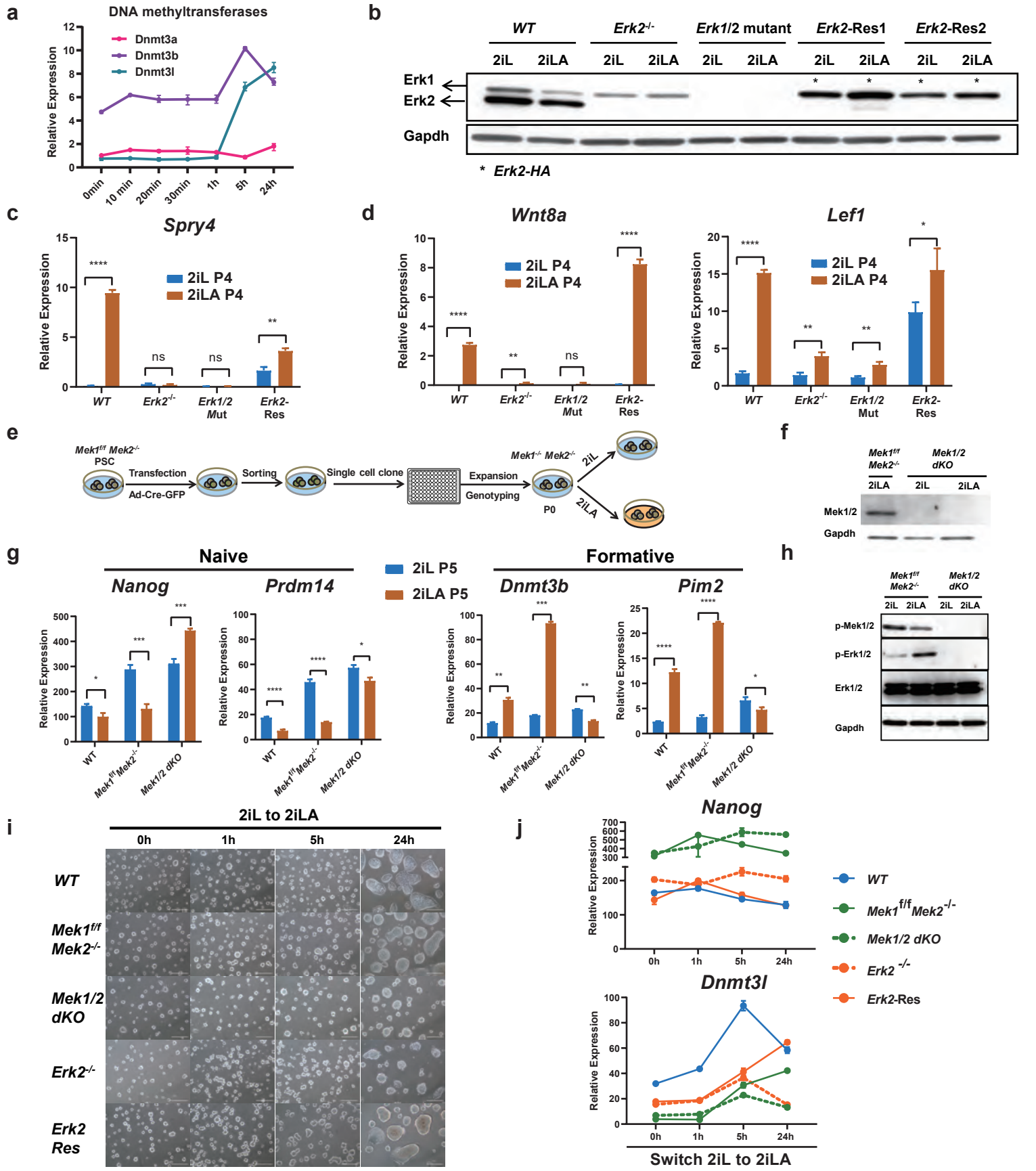

Extended data Fig.7 | Mek/Erk signaling is essential for lipid induced formative transition. a, qRT-PCR for Dnmts transcript levels in ESCs after switching 2iL to 2iLA at different time pionts. **b,** Western blotting for Erk1/2 in *WT*, *Erk2*$^{-/-}$, *Erk1/2* mutant, *Erk2*-Res1 and *Erk2*-Res2 ESCs in 2iL or 2iLA. *Erk2*-Res: *Erk2*-rescued in the *Erk1/2* mutant ESCs (Lentiviral-based shRNA against *Erk1* in the *Erk2* $^{-/-}$ ESCs). **c-d,** qRT-PCR for the Erk1/2 target gene *Spry4*(**c**), and the formative marker genes *Wnt8a* and *Lef1* for *WT*, *Erk2* $^{-/-}$, *Erk1/2* mutant and *Erk2*-Res ESCs after 4 passages cultured in 2iL or 2iLA(**d**). **e-f,** Schematic illustration of the *Mek1/2* dKO ESCs gerneration and the experimental design(**e**), and Western blotting for validating the deletion Mek1/2 protein of the *Mek1/2* dKO ESCs cultured in 2iL or 2iLA (**f**). **g,** qRT-PCR for the naive genes *Nanog, Prdm14* and formative genes *Dnmt3b*,*Pim2* for *WT*, *Mek1*$^{f/f}$*Mek2*$^{-/-}$, *Mek1/2* dKO ESCs after 5 passages in 2iL or 2iLA. *P<0.05,**P<0.01, ***P<0.001, ****P<0.0001, t-test. **h,** Western blotting for the p-Mek1/2 or p-Erk1/2 protein level in *Mek1*$^{-/-}$*Mek2*$^{-/-}$ dKO and its control PSCs. **i-j,** Colony morphology change (**i**) and qRT-PCR for naive gene *Nanog* and formative gene *Dnmt3l* (**j**)after swtiching 2iL to 2iLA at different time pionts for *WT*, *Mek1*$^{f/f}$*Mek2*$^{-/-}$, *Mek1/2* dKO, *Erk2*$^{-/-}$ and *Erk2*-Res ESCs.

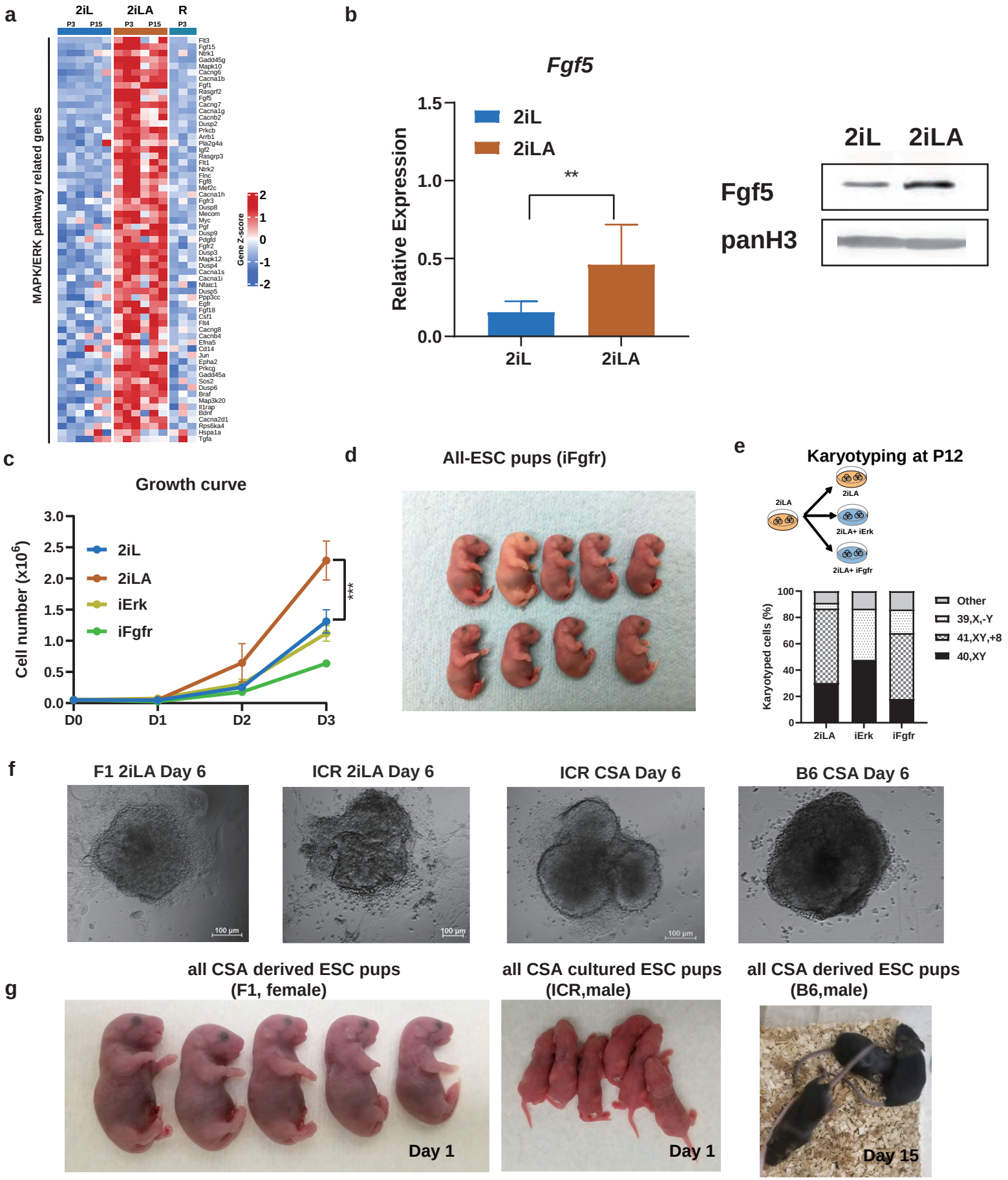

Extended data Fig.8 | Fgf/Erk signaling manipulation in AX-based media maintain the full potency for both sex ESCs. a, Heatmap showing transcript levels of the MAPK/ERK pathway related genes based on bulk RNA-seq for ESC cultured in 2iL or 2iLA at P3. Three biological replicates. **b,** qRT-PCR or Western blotting assays (P3) of Fgf5 for ESC cultured in 2iL or 2iLA. **P<0.01, student t-test. **c,** The growth curve for the proliferation rates for ESCs cultured in 2iL, 2iLA, 2iLA+iErk, or 2iLA+iFgfr media. **d,** Shown are nine pups derived from all ESCs cultured in 2iLA+iFgfr1-3 from one surrogate recipient mouse (9 pups/ 20 embryos transferred) by tetraploid complementation. **e,** Karyotyping analyses of ESCs cultured in 2iLA, 2iLA+iErk, or 2iLA+iFgfr media at P12. **f,** The ICM outgrowth from a F1 (129B6) or ICR E3.5 embryo on feeders at day 6 cultured in 2iLA or CSA. **g,** All-ESC pups generated for the CSA derived ESCs from F1 or B6 E3.5 blastocysts, and for CSA cultured ICR ESCs.

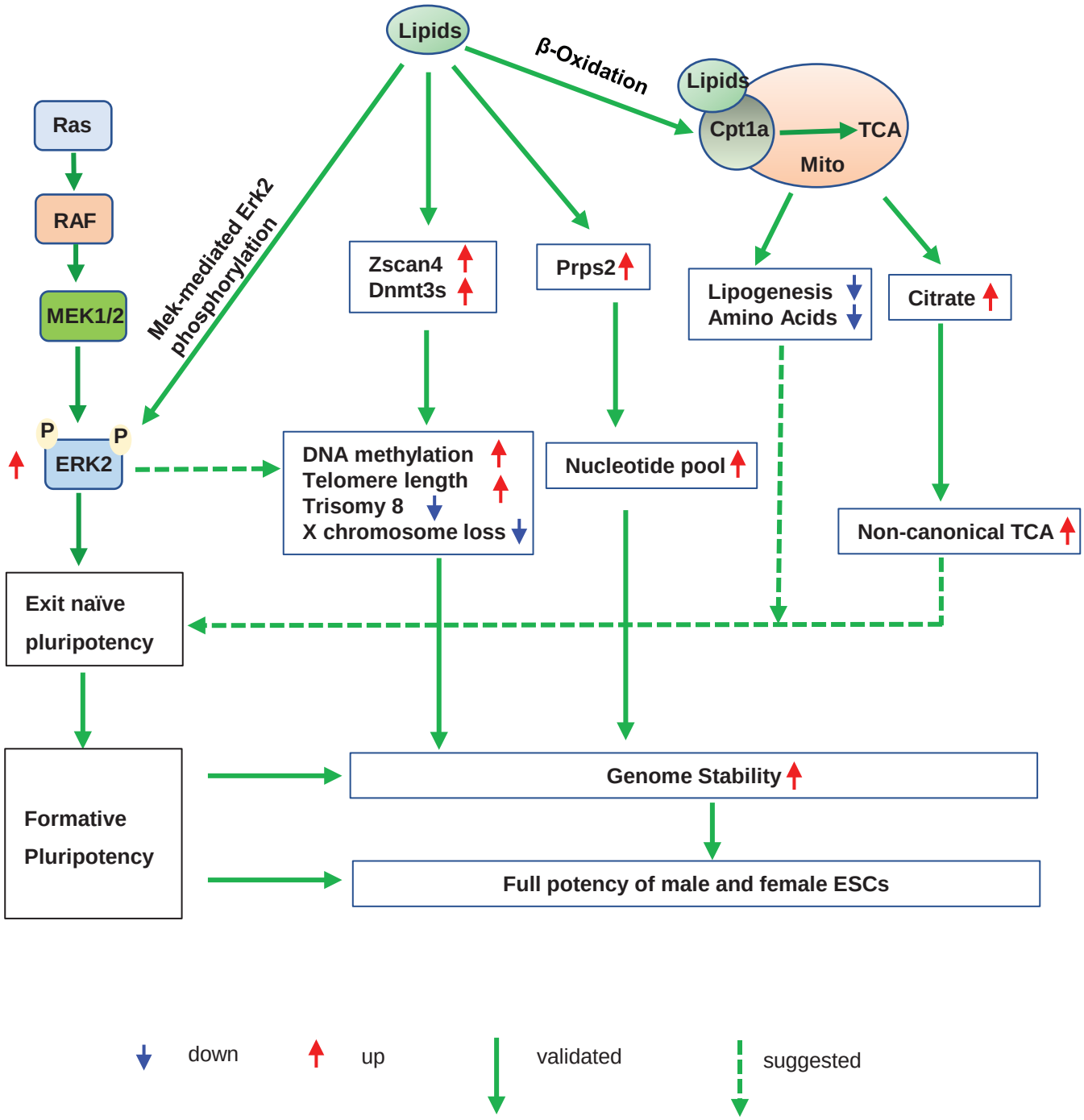

Extended data Fig.9 | Schematic illustrating the dual role of lipids on genome stability and pluripotency of mouse embryonic stem cells. The cytoplasmic lipids directly stimulate Mek-mediated Erk2 phosphorylation which led to exit of naïve state and establish formative pluripotency for ESCs cultured in 2iLA medium. Lipid metabolism through β-Oxidation is dispensable for transition from naïve to formative state, which also reduces the lipogenesis and amino acid biosynthesis and promotes non-canonical TCA metabolites associated with exit of naïve pluripotency. Lipid metabolism promotes nucleotide pool and enhances the expression of Zscan4 and Dnmt3s that are involved in maintenance of telomere length and DNA methylation, therefore improves genome stability during long-term culture. Stimulated Erk2 activity by lipids also alleviates X chromosome loss and trisomy 8 for ESCs cultured in 2iL medium. The dual role of lipids on genome stability and pluripotency facilitates the preservation of full developmental potency of mouse ESCs for both sexes during long-term culture in vitro.